Controlling pedestrian flows with moving walkways

Nicholas Molyneaux * Michel Bierlaire *

February 18, 2021

Report TRANSP-OR 210218
Transport and Mobility Laboratory
School of Architecture, Civil and Environmental Engineering
Ecole Polytechnique Fédérale de Lausanne
transp-or.epfl.ch

*École Polytechnique Fédérale de Lausanne (EPFL), School of Architecture, Civil and Environmental Engineering (ENAC), Transport and Mobility Laboratory, Switzerland, {nicholas.molyneaux, michel.bierlaire}@epfl.ch

Abstract

Moving walkways are pedestrian dedicated hardware which generally decrease pedestrian travel time. We propose the utilization of these devices to dynamically control pedestrian flows in order to improve pedestrian dynamics. Three variations of a control strategy which use moving walkways are proposed in the context of a dynamic pedestrian management system. In this paper, we discuss how a control strategy based upon either historical data, real-time data or predicted data can improve pedestrian dynamics. After analysing whether moving walkways as a control strategy are beneficial for pedestrians, focus is given towards the advantages of the predictive algorithm over the reactive (real-time) algorithm. Next, we discuss which metrics are relevant for inclusion into the multi-objective function of the optimization framework used by the predictive algorithm. The simulation results show that the predictive algorithm is generally fairer across different population groups and is better at preventing high congestion. Furthermore, the predictive algorithm can significantly decrease the travel time compared to the reactive and reference scenarios. The results from the rolling horizon optimization emphasize the trade-off which must be made between travel time and density. Finally, these results confirm the need for control strategies which are tailored to pedestrian flow dynamics.

Keywords Dynamic pedestrian management, model predictive control, moving walkways, pedestrian flow control.

1 Introduction

Controlling and managing pedestrian flows is one approach for improving pedestrian dynamics and preventing hazardous congestion. Control strategies have been applied for decades in road traffic but have only recently been considered for pedestrian traffic. Various combinations of hardware and algorithms ranging from static offline measures all the way to simulation-based predictive management schemes are used. The success of these methods relies upon calibration to the local contexts and exploiting the specific aspects of road traffic. Therefore, pedestrian control strategies must also consider the specificities of walking dynamics. A successful control strategy is not only some hardware installed in a pedestrian walking environment. These flow management schemes generally live inside a larger framework: a dynamic pedestrian management system (DPMS). Such systems are needed for implementations where operators must deal with data collection or state estimation and prediction for example. An extensive discussion about pedestrian management systems is presented in Molyneaux et al. (2019). The authors concluded that transposing strategies from car traffic to pedestrian traffic without addressing pedestrian traffic specificities leads to poor improvement of the pedestrian dynamics. The development of strategies tailored to pedestrian traffic is therefore required to observe substantial benefits.

Pedestrian traffic is challenging and complex since individuals are free to move in any direction at any time. This freedom means that bidirectional flow occurs often. Furthermore, complex interactions take place in junctions where pedestrians use different sub-routes to reach their destination. Therefore, improving pedestrian dynamics can be achieved by preventing, or reducing, bidirectional flow. Further improvements can be expected if pedestrian density is kept low inside junctions where pedestrians move in many different directions. By addressing these two elements, a control strategy should have the potential to decrease pedestrian travel time and improve walking speed.

In this paper, we propose the use of dynamically controlled moving walkways to reduce congestion and decrease pedestrian travel time. One advantage of such hardware is that pedestrians already use them in many different contexts. We present different flavours of a control strategy which uses moving walkways to improve the pedestrian dynamics. Three variations are proposed: one based upon historical data, one reactive strategy, and one predictive strategy. These three control algorithms are analysed and the effect of them upon pedestrian travel time and density is discussed. We discuss three research questions. Firstly, we investigate whether moving walkways can be used to improve pedestrian flows. Secondly, we analyse the benefits of including short-term predictions into the control strategy, as opposed to schemes using only historical or real-time data. The third and final hypothesis concerns the predictive scheme: we discuss whether multi-objective optimization can be used inside pedestrian specific flow control

schemes. The predictive algorithm relies upon an optimization framework to minimize a defined objective function by searching for the best speed profile of the moving walkways in the short-term future. To achieve this, an objective function relying on a combination of pedestrian centric metrics must be defined. The choice of metrics included in the objective function is discussed, alongside their impact on the pedestrian dynamics. This optimization procedure is computationally expensive, hence it's added value must be evaluated.
The following section discusses the literature on dynamic control strategies for pedestrians and the major contributions in road traffic control strategies. After that, we present the three control algorithms and the required input data. Next, we present the results from two case studies where we simulated the installation of moving walkways. The three control algorithms are tested and their effects on the pedestrian dynamics are discussed before concluding this article.

2 Literature review

The first element we discuss in the literature are the applications of moving walkways linked with pedestrian flows. Then, we cover dynamic pedestrian control strategies for pedestrian traffic in the literature. Following this, we cover major contributions and elements in road traffic control strategies to summarize the important paradigms which have been proposed in the literature.

Moving walkways Mechanical and geometric considerations for speed, acceleration, capacity, etc. of moving walkways are provided in Scarinci et al. (2017). The authors discuss the benefits of installing moving walkways to move pedestrians around at a city level. They propose accelerated moving walkways as a transportation mode. An optimization framework which analyses the trade-off between installation cost and benefit is used. Furthermore, many practical considerations are discussed concerning the installation constraints.
Although moving walkways are common inside airports, few studies consider these devices outside of their usual context as a transportation mode. Moving walkways can be considered in the context of "Smart cities" to decarbonate individual transport inside cities. Furthermore, a trend towards improving walkability of cities means pedestrian demand might increase in the coming decades. (Fonseca et al., 2020).

Pedestrian control strategies Managing pedestrian flows is important in many different contexts. One area where pedestrians generally wish to move freely and reach their destination as fast as possible is transportation hubs . Passenger flow control is therefore important to achieve this goal (Shang et al., 2019). Pedestrian flow through doors is analysed at a very small scale in Seriani and Fernandez

(2015) where the authors simulated the movement of pedestrians in and out from public transport vehicles. The authors focused on the static design of hardware like handrails near the doors. In Wang et al. (2013), the authors show that simulation tools can be used to prevent high congestion and hazardous situations. A feedback control scheme based upon an aggregate pedestrian motion model is proposed in Zhang and Jia (2021) where the authors control pedestrian flow to prevent excessive congestion in corridors. The inflow into urban rail stations is controlled in Jiang et al. (2018) by using buffer zones in front of the doors. In Xu et al. (2016), the authors provide a general framework which can help operators decide whether local passenger flow control should be applied. Nevertheless, no system-wide short-term predictions are used to provide future state data. Passenger flow control is considered at a train network level where the trade-off between train usage and waiting passengers is explored (Liu et al., 2020a). Although control strategies for pedestrian flows is getting more attention nowadays, most strategies rely upon a reactive scheme and the added value of short-term predictions is yet to be explored.

Pedestrian safety during large events is obviously critical. This question has also been addressed with flow control measures. Pedestrian flow control is applied in the Mecca (Saudi Arabia) during pilgrimage. A reactive policy is applied to reduce inflow to prevent excessive congestion and hazardous situations. Again, no online predictive control policy is applied (Abdelghany et al., 2016). The design of static checkpoints for large events is explored in Aros-Vera et al. (2020). Pedestrian flow is controlled in a reactive way in Zhang et al. (2016) where the authors use a macroscopic model to simulate the movements of pedestrians. The assumptions about homogeneity on the links are hard to satisfy in practice.

Although the analysis of pedestrian movements of boarding and alighting flows around public transport vehicles and safety aspects during large events have been studied, no predictive control strategy focusing on daily operations is available. To the best of our knowledge, moving walkways have never been considered as a control device for managing pedestrian flows in a predictive way.

Road traffic control strategies Without presenting all possible road traffic control strategies, we will discuss the major paradigms which can be found in the literature. Control strategies are adapted to the general context like freeways, urban networks, or route guidance for example (Papageorgiou et al., 2003). Maybe the most common control strategy for freeways is ramp metering (Papageorgiou et al., 1991). Today, many different flavours of the original control strategy are available: reactive versions which exploit traffic flow measurements (Ben-Akiva et al., 2003; Abuamer et al., 2016) or predictive versions which use short-term predictions (Bellemans et al., 2006; Roncoli et al., 2016) are common in the literature.

The classical example of urban traffic control is signalized intersections. Two cat-

egories of strategies exist: fixed-time strategies and traffic responsive strategies. The first is calibrated offline based on historical data while the second adapts the phases based upon traffic flow measurements. Similarly to ramp metering, traffic responsive control strategies for lights can be reactive or predictive, and/or isolated or coordinated (Papageorgiou et al., 2003). Recent work on signalized intersections includes fuel consumption analysis and autonomous (or connected) vehicle integration into the strategies (Zhou et al., 2020; Tang et al., 2018).
Through these few examples, we see that control strategies for road traffic are firstly tailored to specific problems which occur in road traffic like intersections or lane merging. Secondly, control strategies can be categorized into three groups: fixed, reactive, and predictive. Fixed strategies are designed offline based upon historical data. Reactive strategies adapt the control measures based upon real-time traffic conditions. Predictive strategies exploit a model to gain insight into the traffic conditions which are going to occur in the near future.

3 Moving walkways as a control strategy

In this paper, we discuss the feasibility of using moving walkways as a control strategy. Moving walkways as control devices have the potential of influencing the pedestrian flows since the speed and direction of these devices can change over time. To the best of our knowledge, moving walkways (MW) have not yet been used by a dynamic control strategy. We present and discuss the major elements which are needed to design a control algorithm using these devices. We propose three different flavours of the control algorithm: a fixed (or static), a reactive and a predictive version. Although many implementation details must be considered to use the control devices in practice, such considerations are beyond the scope of this paper in which we analyse the benefits of using such devices on the pedestrian dynamics. Nevertheless, some assumptions must be made in order to design control algorithms which are feasible in practice. We start by presenting and discussing these assumptions.
The walkable environment in which the moving walkways can be used as control devices must be one where pedestrians wish to reduce their travel time and avoid congestion. Train stations during the peak hours are a typical example. Pedestrians already use moving walkways in airports to travel long distances or inside shopping malls to change floors for example. Therefore, an advantage of moving walkways compared to other novel technologies is the user acceptance. Users will not be exposed to a new technology, hence no learning phase is required. This leads to the first assumption concerning compliance. We assume that the pedestrians respect the direction of the moving walkway. Secondly, we assume that pedestrians walk while on the moving walkway.
The following assumptions concern the devices themselves. We assume that the speed of a moving walkway must be selected from a discrete and predetermined

set of speeds. Note that the speed may be signed, so that the walkway can be operated in two directions. The speeds are considered discrete for safety and comfort reasons. Safety issues will arise if the speed of the MW changes continually. Furthermore, a pedestrian who is standing on the MW will feel uncomfortable if every few seconds the speed increases or decreases. If individuals don't feel safe on the devices, then user acceptance will be low and they will prefer to walk instead. When a MW changes direction, a buffer time must be given to the pedestrians to clear the device before it changes direction. This buffer time should be long enough such that an individual who has just entered the MW can leave it before the MW changes direction. Furthermore, during this buffer time, no pedestrians should be allowed to enter the MW. Although the MW can change direction at any time to move in the same direction as the larger pedestrian flow, the direction should not change too often. The assumptions about the speed discretization and buffer time will be formally defined in the following paragraphs.

At a tactical level, the installation of moving walkways adds another alternative path pedestrians can choose from. Each individual must now choose from walking or using the moving walkway to reach his next intermediate destination. Therefore, two parallel flows of pedestrians between two locations can exist: one walking and one using the MW.

The two assumptions regarding compliance raise challenging practical and safety questions. User compliance towards the direction is generally respected in practice. On the other hand, the assumption where no pedestrians enter the moving walkway during the clearing buffer time before a direction change is more delicate. To prevent pedestrians from entering the MW, a clear means of information or physical obstruction needs to be used. The use of a physical obstacle (such as a gate) may raise safety issues, while the absence of such an obstacle may generate a lack of compliance. These practical issues are not discussed further in this paper.

Before advancing to the input requirements of the control algorithm, we clarify some terminology. A *control strategy* can be decomposed into three major elements:

Control devices: Hardware used to apply the control strategy, in this case moving walkways.

Control algorithm: Equation or function which defines the state of the control devices based upon measured and simulated data.

Control configuration: Set of variables generated from the control algorithm and applied using the control devices. In the present case, the speeds of the moving walkways.

We define the following notation concerning the temporal and spatial representations. A specific moment in time (a snapshot) is denoted t, while a time interval $[t_{start}, t_{end}]$ is denoted by τ. The walkable environment in which the pedestrians

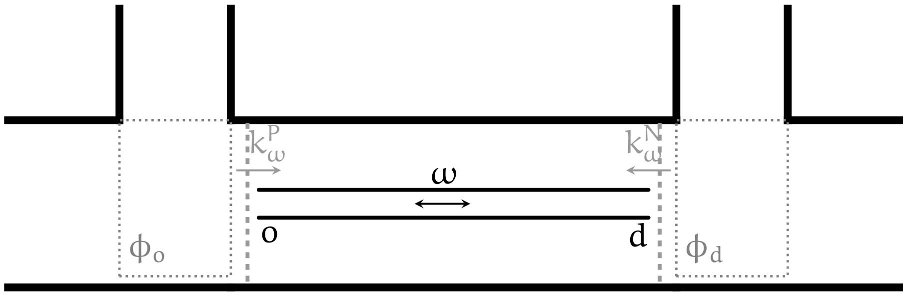

Figure 1: Schematic presentation of a moving walkway.

can move around is denoted L, while a specific sub-element (region or line) is $L' \subset L$. The collection of moving walkways installed in the walkable environment is $\mathcal{W}$. Each moving walkway $\omega \in \mathcal{W}$ has a static origin o and destination d. The area near the origin of the MW is denoted ϕ_o and the area at the end is ϕ_d. The speed of a given walkway ω during the time interval $\tau = [t, t + \Delta t_s]$, where Δt_s is time interval length, is $s_\omega(\tau)$. The speed of the MW cannot change during the interval τ. It is positive if the direction of movement is going from ϕ_o to ϕ_d, and negative if moving from ϕ_d to ϕ_o. The set of possible speeds is $\mathcal{S}$, hence $s_\omega(\tau) \in \mathcal{S}$. The maximum speed of moving walkways is $s^{max} = 3m/s$ in practice (Scarinci et al., 2017). An example of a MW installed in a corridor is shown in Figure 1.

3.1 Control algorithm input

The control strategy, more specifically the different control algorithms, require input data to generate the control configurations. The control strategy we propose uses three different quantities: pedestrian flow, density and travel time.

The pedestrian flow $k(L', \tau)$ is the number of pedestrians who enter the area or cross the line L' during time interval τ. For a given moving walkway ω, we define two parallel flows (one per direction) as the pedestrian flows which are using ω or that could use ω. Therefore, for each MW, we define k_ω^P and k_ω^N as the flows moving in the positive, respectively negative, direction of ω. Figure 1 presents both parallel flows. All pedestrians crossing the grey dashed lines are those counted in the "parallel flows".

The pedestrian density inside area L' at a given time t is denoted by $\rho(L', t)$. The spatial context L' can be a corridor or junction linking corridors for example. The density threshold above which we consider congestion takes place is ρ^c.

The travel time of individual n is denoted tt_n. The travel time is defined as the duration the pedestrian spent inside the spatial context L between when he enters until when he leaves.

The different flavours of the control algorithms need different temporal contexts of the quantities. The collection of quantities of interest (flow or density for example) is denoted Δ. For any fundamental quantity of interest, we define the

historical, real-time, and predicted counterparts. Historical versions are denoted $\cdot^{H}$, real-time versions are denoted $\cdot^{*}$ while predicted values are denoted $\cdot^{+}$. The historical data is collected over the previous days, months or years. Real-time data is collected using measurement devices in the very short-term past like the previous few minutes or seconds. Predicted data covers the short-term future. Since the predicted data is uncertain by nature, the predicted data is provided as distributions of the quantities. This allows the control algorithm to exploit the uncertainty of the forecast and potentially give more weight to predicted quantities with less variance.
In this paper, the empirical distributions are generated from R replications of the short-term predictions accomplished using a simulator. We assume that the quantities generated by the simulator are unbiased. Furthermore, we assume that the variance in the quantities does not vary over the prediction horizon.
The different quantities of interest, for both the real-time and predicted time contexts, are provided by frameworks called dynamic pedestrian management systems (DPMS). The systems use state estimation and state prediction to generate the data. We assume that such a system is available to provide the data. A DPMS is the pedestrian tailored counter part of road traffic DTMS (Molyneaux et al., 2019). The details of the DPMS implementation are described in the case studies.

3.2 Control variables

For a collection of moving walkways installed in an infrastructure, the control variables are the speeds of each moving walkway. For a time period T decomposed into intervals of equal duration Δt_s, the control configuration is:

$$\mathcal{C}_\omega(T) = \{s_\omega(\tau)\} \quad \forall \tau \in T, \tag{1}$$

where $s_\omega(\tau)$ is the speed of walkway ω over interval τ. The speed at the end of interval $\tau_i = [t_i, t_i + \Delta t_s]$ can change to any value within S for the next interval $\tau_{i+1} = [t_i + \Delta t_s, t_{i+1} + 2\Delta t_s]$. The speed transition phase (or acceleration/deceleration phase) takes place at the beginning of τ_{i+1}. Therefore the new speed is only applied after the transition time. The acceleration of moving walkways is $0.25 m/s^2$ (Scarinci et al., 2017). An example speed profile with the acceleration phases is shown in Figure 2. The transition between the first interval $[0, 10]$ and the second interval $[10, 20]$ lasts four seconds since the speed difference is $1 m/s$ and the acceleration is $0.25 m/s^2$. The speed profile includes the acceleration/deceleration phases such that the configuration is enforced at the end of each interval.

Time [s]	Speed [m/s]
0-10	3.0
10-20	2.0
20-30	0.0
30-40	-2.0
40-50	-2.0
50-60	-1.0

(a) Control configuration

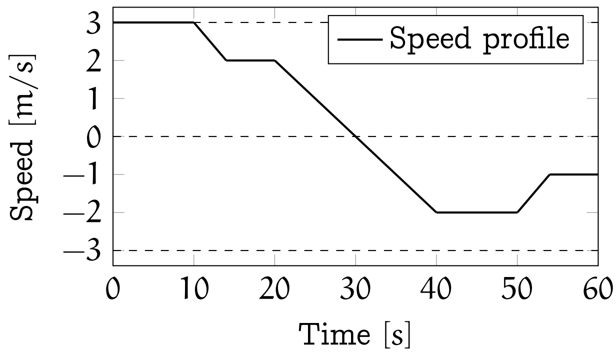

(b) Moving walkway speed profile example

Figure 2: Control configuration example for a moving walkway with the corresponding speed profile.

4 Control algorithms

Maybe the most challenging aspect of designing a new control strategy is the development and calibration of the control algorithms. The algorithm links the fundamental data to the control configuration of the devices. With this paper, we aim to investigate whether moving walkways are beneficial for pedestrians. Furthermore, we discuss whether predictive control shows a significant improvement over reactive control. To achieve this, we propose three variations of the control algorithms. The first is a fixed (or static) approach, the second a reactive algorithm and the third a predictive algorithm. These three control algorithm flavours generate the control configuration based upon input data:

$$\mathcal{C}_{\mathrm{f}} = \mathcal{F}_{\mathrm{f}}\left(\Delta^{\mathrm{H}}\right) \tag{2}$$

$$\mathcal{C}_{\mathrm{r}} = \mathcal{F}_{\mathrm{r}}\left(\Delta^{*}\right) \tag{3}$$

$$\mathcal{C}_{\mathrm{p}} = \mathcal{F}_{\mathrm{p}}\left(\Delta^{*}, \Delta^{+}\right) \tag{4}$$

where $\mathcal{C}_{\mathrm{f}}$, $\mathcal{C}_{\mathrm{r}}$ and $\mathcal{C}_{\mathrm{p}}$ are the fixed, reactive and predictive control configurations. $\mathcal{F}_{\mathrm{f}}$, $\mathcal{F}_{\mathrm{r}}$ and $\mathcal{F}_{\mathrm{p}}$ are the fixed, reactive and predictive control algorithms. The fixed algorithm exploits historical data. The reactive algorithm exploits real-time data and the predictive algorithm exploits predicted data. The predictive algorithm needs the real-time data to generate the predictive data. Figure 3 presents the temporal notations for all three control algorithms. The algorithms which are presented in the following sections exploit pedestrian flow and pedestrian density to generate the control configurations.
All three algorithms share a common goal: they aim at moving pedestrians as fast as possible to their destination. The total travel time of all pedestrians (system optimum) is minimized, not the pedestrian specific travel times (user optimum). This objective must be balanced with congestion since transporting many pedestrians into the same area of the infrastructure can lead to hazardous congestion.

Therefore, a trade-off between minimizing travel time and minimizing congestion must be addressed.

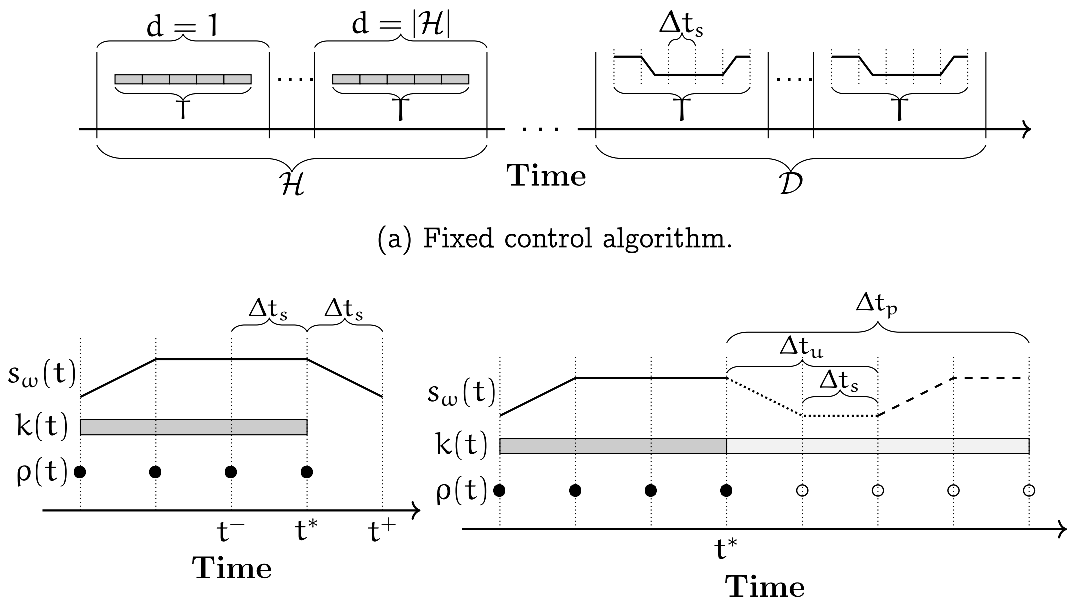

(a) Fixed control algorithm.

(b) Reactive control algorithm.

(c) Predictive control algorithm.

Figure 3: Temporal contexts and notations for the three control algorithms.

4.1 Fixed control algorithm

A fixed control configuration is generated based upon the average observed flows computed for short time intervals. The idea is to have the moving walkways carrying pedestrians in the same direction as the maximum observed average pedestrian flow in each time interval. The speed of the moving walkway is set to the fastest value from $\mathcal{S}$. For example, let's consider the morning peak hour between 7:00 and 8:00 and one single moving walkway. We discretize this time period into 5-minute intervals and compute, for each interval, the average over the historical data of the pedestrian flow in each direction of the MW. Then, for each time interval, the direction of the moving walkway is set to match the maximum average flow. This example is formalized in the following paragraphs.

The input data consists of a historical data set $\mathcal{H}$ composed of data covering the same time period T (the morning peak hour for example), indexed by d. The control configuration, generated by the fixed control algorithm, will be used for the set of days $\mathcal{D}$. The time period under consideration T is divided into intervals of length Δt_s. The temporal context for the fixed control algorithm is presented in Figure 3a. The average observed parallel flows for each moving walkway is computed for each interval $\tau \in T$:

$$\overline{k^{P}_{\omega}}(\tau) = \frac{1}{|\mathcal{H}|}\sum_{d\in\mathcal{H}} k^{H,P}_{\omega,d}(\tau), \quad \overline{k^{N}_{\omega}}(\tau) = \frac{1}{|\mathcal{H}|}\sum_{d\in\mathcal{H}} k^{H,N}_{\omega,d}(\tau) \quad \forall\tau \in T, \omega \in \Omega \tag{5}$$

where $\bar{\cdot}$ represents the mean, $k^{H,P}_{\omega,d}(\tau)$ is the observed pedestrian flow moving in the positive direction of ω during interval τ of historical data d. The average parallel flows for each time interval are $\overline{k^{P}_{\omega}}(\tau)$ and $\overline{k^{N}_{\omega}}(\tau)$ in the positive and negative directions. Algorithm 1 presents this fixed control algorithm. The "speed transitions" insert acceleration and deceleration phases, when needed, to have a feasible speed profile (as described in section 3.2).

Algorithm 1: Fixed control algorithm

Input:

time period of interest T

historical data: $k^{H,P}_{\omega}(T)$ and $k^{H,N}_{\omega}(T)$

Control:

compute $\overline{k^{P}_{\omega}}(T)$ and $\overline{k^{N}_{\omega}}(T)$ using (5)

for $\tau \in T, \omega \in \Omega$ **do**
  if $\overline{k^{P}_{\omega}}(\tau) > \overline{k^{N}_{\omega}}(\tau)$ **then**
    $s_{\omega}(\tau) = +s^{\max}$
  else
    $s_{\omega}(\tau) = -s^{\max}$
  end
  insert speed transitions
end

Output: fixed control configuration $\mathcal{C}_f$

4.2 Reactive control algorithm

The second control scenario we propose is a reactive approach. We exploit pedestrian flow and density data collected inside the walkable space to update the direction and speed of the moving walkways dynamically by defining $\mathcal{F}_r$. This control algorithm uses the data provided by the DPMS covering the recent passed to first decide on the direction of the MW based upon pedestrian flow data, then to set the speed according to density data. The direction is decided by considering pedestrian inflow near the extremities of the moving walkway. The direction is set such that pedestrians are carried away from the extremity into which the majority of pedestrians are entering. Then, the speed is set using a proportional-integral (PI) controller regulating density.

The direction and speed of each MW are updated at regular intervals Δt_s. Considering the rapid changes in pedestrian dynamics which can occur, the update interval should be short. This is specially true for the speed, while the direction could be updated less often. The time at which an update is computed (the present time) is denoted t^*. The next update will occur at $t^+ = t^* + \Delta t_s$. The previous update took place at $t^- = t^* - \Delta t_s$. Figure 3b summarizes the temporal context. We recall that the MW speeds are considered constant over time intervals, therefore we define the following notation: τ^- is the interval $[t^-, t^*]$ and τ^+ is the interval $[t^*, t^+]$, hence the MW speed during the previous interval is $s_\omega(\tau^-)$ while the speed during the next interval is $s_\omega(\tau^+)$.
We propose the utilization of a rule based upon pedestrian flow. The direction of the MW for the next interval is set using the following:

$$\text{if } \operatorname{sign}(s_\omega(\tau^-)) = +1 \rightarrow \operatorname{sign}(s_\omega(\tau^+)) = \begin{cases} +1 & \text{if } A \cdot k_{\phi_o}(\tau^-) < k_{\phi_d}(\tau^-) \\ -1 & \text{otherwise} \end{cases} \tag{6}$$

$$\text{if } \operatorname{sign}(s_\omega(\tau^-)) = -1 \rightarrow \operatorname{sign}(s_\omega(\tau^+)) = \begin{cases} -1 & \text{if } k_{\phi_o}(\tau^-) < A \cdot k_{\phi_d}(\tau^-) \\ +1 & \text{otherwise} \end{cases} \tag{7}$$

where $\operatorname{sign}(s_\omega)$ indicates the direction of movement of ω, the parameter A reflects how much the flows must change before the direction changes, $k_{\phi_o}(\tau^-)$ and $k_{\phi_d}(\tau^-)$ are the inflows of pedestrians into areas ϕ_o and ϕ_d during τ^-. This direction update rule is applied only if a direction change is allowed to take place. To prevent excessive direction changes, after a direction change has occurred, we prevent the moving walkway from changing direction again for a given time. The duration while the direction change is prohibited is denoted δ_{dir}. Assume a direction change has taken place at t^*, then the next direction change cannot take place before $t_{dir} = t^* + \delta_{dir}$.
The parameter A allows the operator to influence the balance between changing direction to match the major flow and preventing excessive direction changes. Changing direction as soon as the flow coming in the opposite direction to the MW exceeds by 1% the flow in the same direction of the MW is likely to be counterproductive. The parameter A represents by what fraction the flow coming in the opposite direction must exceed the flow moving in the same direction before changing direction.
Next, we define how the speed is updated at each interval. Similarly to many traffic control methods (Baskar et al., 2011), we propose a speed update rule using a PI controller. We regulate density by controlling the speed of the moving walkway. The PI controller generates speeds which are continuous, hence the speed is rounded to the nearest value found in the set of possible speeds $\mathcal{S}$ before being enforced. Since we aim at preventing excessive congestion at either end of the moving walkway, we provide the PI regulator with a set point: ρ^s. This is the density the regulator targets. The error between the set point and measurement

at time t, monitored in zone ϕ, is denoted $e^{\rho}_{\phi}(t) = \rho^s - \rho(\phi, t)$. Similarly to Tympakianaki et al. (2014), the PI regulator equation linking the speed of the moving walkway ω to the density at the downstream exit is:

$$s_{\omega}(\tau^{+}) = \left\lfloor s_{\omega}(\tau^{-}) - e^{\rho}_{\phi}(t^{*})\left[K_p + K_I\right] + e^{\rho}_{\phi}(t^{-})K_P \right\rceil^{\mathcal{S}} \tag{8}$$

where $\lfloor\cdot\rceil^{\mathcal{S}}$ represents to operation of rounding to the nearest value in $\mathcal{S}$, K_P and K_I are respectively the proportional and integral gains, $e^{\rho}_{\phi}(t^{*}) = \rho^s - \rho_{\phi}(t^{*})$ and $e^{\rho}_{\phi}(t^{-}) = \rho^s - \rho_{\phi}(t^{-})$ are the density errors measured at t^{*} and t^{-}. The regulator tries to drive the errors to 0. The density measurements are taken from the downstream exit. If the MW is moving in the positive direction, then measurements in $\phi = \phi_d$ are used, otherwise, if the MW is moving in the negative direction, then measurements are taken in $\phi = \phi_o$. The complete control algorithm is presented in Algorithm 2.

Algorithm 2: Reactive control algorithm.

Input:

parameters: $A, \delta_{dir}, K_P, K_I$

flow and density data: Δ^{*}

Control:

for $\tau^{+} = [t^{*}, t^{*} + \Delta t_s]$ **do**

  for $\omega \in \Omega$ **do**

    if $t^{*} > t_{dir}$ **then**

      update direction using (6) and (7)

      update $t_{dir} = t^{*} + \delta_{dir}$

    end

    update $s_{\omega}(\tau^{+})$ using (8)

  end

  insert speed transitions

end

Output: updated speed and direction for all MW

4.3 Predictive control algorithm

The final control algorithm we propose exploits short-term predictions of the pedestrian dynamics. Therefore, we define $\mathcal{F}_p$ which exploits Δ^{*} and Δ^{+} to generate the control configuration. The rolling horizon paradigm allows the specification of a control configuration for the short-term future by exploiting predictions of the demand and quantities of interest. The predictions are accomplished using a pedestrian simulator. The current state data Δ^{*} is collected thanks to measurement devices and completed using state estimation. Then, state prediction generates the data for the near future Δ^+. The duration of the prediction horizon is denoted by Δt_p. The prediction horizon $T^+ = [t^*, t^* + \Delta t_p]$ is discretized into intervals of length Δt_s. The temporal context can be found in Figure 3c. The speed of each MW for each interval in the prediction horizon is the control configuration. The specification of the control configuration is accomplished by minimizing an objective function computed from predictions of the quantities of interest Δ^+ by using an optimization algorithm. The key assumption under which the optimization problem is relevant is that the quantities of interest (travel time, density, flow) depend on the speed and direction of the moving walkways. The optimal control configuration is applied until it gets updated. The predicted control configurations are updated at regular intervals Δt_u. This procedure is summarized in Algorithm 3.

The decision variables of the optimization problem are the control configurations of each moving walkway. We recall that the speeds are discretised in time and magnitude. The decision variables are therefore the collection of all speeds of all moving walkways:

$$s = \{s_\omega(\tau)\} \quad \forall \tau \in T^+, \omega \in \mathcal{W}, \tag{9}$$

with $s_\omega(\tau) \in \mathcal{S}$ since the speeds are discrete. The optimal control configuration is denoted s_{opt}. Two versions of the predictive algorithm are proposed which differ by using different optimization algorithms. The first is a single objective variation and the second is a multi-objective variation.

Algorithm 3: Predictive control algorithm.

Input:

flow, density and travel time data: Δ^* and Δ^+

optimization algorithm: $\mathcal{O}$

Control:

for $T^+ = [t^*, t^* + \Delta t_p]$ **do**
  find optimal configuration s_{opt} using $\mathcal{O}$

end

apply s_{opt} until update at $t_u = t^* + \Delta t_u$

Output: optimal control configuration over T^+

4.3.1 Single objective predictive algorithm

The objective function is computed from the predicted state data Δ^+. We consider travel time as the objective to minimize. The mean travel time of all pedestrians inside the simulation environment is used to take travel time into consideration:

$$\chi^{T^+}(s) = \frac{1}{|N|} \sum_{n \in N} tt_n(s) \tag{10}$$

where $tt_n(s)$ is the travel time of pedestrian n which depends on the control configuration s and N the collection of pedestrians inside the simulation. Since the short-term predictions rely on a pedestrian simulation which is stochastic, we perform R replications of the short-term prediction at each evaluation of the objective function to build distributions of the indicator. We then compute the mean value from these distributions to evaluate the objective function:

$$\overline{\chi^{T+}}(s) = \frac{1}{|R|} \sum_{r \in R} \chi_r^{T+}(s). \tag{11}$$

The optimization problem which the predictive control algorithm must solve at each iteration of the rolling horizon scheme can therefore be written as:

$$\begin{aligned} s_{opt} = \arg\min_{s} \quad & \overline{\chi^{T+}}(s) \\ \text{s.t.} \quad & s \in \mathcal{S} \end{aligned} \tag{12}$$

The predictive control algorithm solves the optimization problem (12) each time the configuration is updated. Considering the discrete nature of the decision variables and the simulation-based objective function, we propose the utilization of the adaptive large neighbourhood search algorithm for solving (12). This algorithm is flexible since it can handle single and multi-objective problems (Ropke and Pisinger, 2006).

Adaptive large neighbourhood search Adaptive large neighbourhood search (ALNS) is meta-heuristic optimization algorithm which uses a collection of heuristics (operators) to generate new solutions from an existing one. The original algorithm is adapted to include the acceptance criteria from simulated annealing (Gendreau et al., 2010). This reduces the risk that the algorithm gets trapped in local minima. Algorithm 4 shows the complete algorithm.

Operators A collection of operators $\mathcal{O}$ is used to generate new solutions from the current solution. They have been developed specifically for the purpose of optimizing the control configuration of moving walkways. One operator $o \in \mathcal{O}$ is selected at each iteration. This operator is selected using the adaptive weights method proposed in Ropke and Pisinger (2006). At iteration i, the current solution x^i is transformed using operator o to generate the next solution: $x^{i+1} = o(x^i)$. The collection of operators is presented below. The operators are described assuming only one MW is available for the sake of clarity. Each operator has a parameter, denoted α, which controls the distance between x^i and x^{i+1}.

Increase speed A randomly sampled fraction $\alpha \in [0.2, 0.8]$ of the decision variables are increased. The fraction of decision variables to change is equal

Algorithm 4: Single objective ALNS using the simulated annealing selection criteria.

Input:
feasible solution: x
operator set: Θ
Initialization:
operator weights: g
iteration counter: $i = 0$
maximum number iterations: n
random number generator: r
temperature: T
best solution: $x^b = x$
current solution: $x^i = x$
Iterations:
while $i < n$ **do**
  select operator $o \in \Theta$ using g
  $x^{i+1} = o(x^i)$
  if $c(x^{i+1}) < c(x^b)$ **then**
    $x^b = x^{i+1}$
  else if $\frac{\exp(c(x^{i+1}) - c(x^b))}{T} > r$ **then**
    $x^b = x^{i+1}$
  else
    reject x^{i+1}
  end
  update g
  decrease T
  $i = i + 1$
end
Output: best solution x^b

to α. Then, the speed is increased to the next discrete value. For example, for $x^i = [2, 2, 1, 0, -1, -2]$ and a fraction to change $\alpha = 0.5$, then $x^{i+1} = [3, 3, 1, 0, 0, -2]$.

Decrease speed Analogous to the previous operator, except that the speeds are decreased to the next discrete value. For example, for $x^i = [2, 2, 1, 0, -1, -2]$ and a fraction to change $\alpha = 0.5$, then $x^{i+1} = [1, 1, 1, 0, -1, -3]$.

Accelerate A fraction $\alpha \in [0.2, 0.8]$ of the speeds is selected and their amplitude is increased. The moving walkways are moving pedestrians faster after this operator. For example, for $x^i = [2, 2, 1, 0, -1, -2]$ and the fraction to change $\alpha = 0.5$, the next solution becomes $x^{i+1} = [3, 3, 1, 0, -2, -2]$.

Slow down Analogous to the previous operator, this operator slows down a fraction of the control configuration. For example, for $x^i = [2, 2, 1, 0, -1, -2]$ and the fraction to change $\alpha = 0.5$, the next solution becomes $x^{i+1} = [1, 1, 1, 0, 0, -2]$.

Direction matches flow Each MW is selected with probability $\alpha = 0.5$. For each moving walkway which has been selected, the direction is set to be the same as the largest predicted parallel flow of that MW. The magnitude of the moving walkway speed is set to fastest value. This operator is combined with the "Decrease speed" and "Increase speed" operators to induce variability in the solution.

Change direction A randomly selected fraction $\alpha = [0.2, 0.8]$ of the control configuration changes direction, but keeps the speed amplitude. For example, for $x^i = [2, 2, 1, 0, -1, -2]$ and a fraction to change $\alpha = 0.5$, then $x^{i+1} = [-2, -2, 1, 0, 1, -2]$.

Density comparison The direction of the moving walkway is set such that it moves pedestrians from high density to low density. This way it tends to reduce congestion in the more congested areas of the infrastructure. Each moving walkway is selected with a probability $\alpha = 0.5$.

Random speed Each MW is selected with a probability $\alpha = 0.5$. For each selected MW, set a randomly selected constant speed for all time intervals. After that, the "Decrease speed" and "Increase speed" operators are applied to induce variability in the solution.

Resample best solution This operator will add replications to the existing best solution in order to increase confidence in the computed indicators.

Both the "accelerate" and "increase speed" operators help the ALNS algorithm in the solution space exploration. The "accelerate" operator makes MW move faster, hence positive speeds are more positive, while negative speeds are more negative. On the other hand, the “Increase speed” operator moves speeds closer to the positive upper bound. The ”Accelerate“ operator is useful for exploring the high speed solutions, while the “Increase speed” helps explore the intermediate speed solutions. When moving walkway operators must be selected, the selection probability is fixed to 50% ($\alpha = 0.5$). This choice is made to guarantee that the operator has a reasonable probability of changing the control configuration without entirely changing the configuration. With a low MW selection probability, the operator would often return the same control configuration, and for a high MW selection probability, the operator would return a completely different control configuration.

4.3.2 Multi-objective predictive algorithm

The single objective predictive control algorithm considers only travel time as an objective. Monitoring only travel time can lead to unbalanced dynamics inside the infrastructure. For example, one corridor intersection could present very high congestion, hence acting as a barrier preventing some pedestrians from moving, while giving the other users ample space to reach their destinations. To prevent such unfair, and possibly dangerous situations, we propose a second variant of the predictive control algorithm which uses a multi-objective optimization algorithm (Alg. 5). We define two new objectives and keep travel time as well (eq. 10). The first is average pedestrian congestion inside a collection of regions Φ within the walkable environment. Congestion is incorporated by integrating over the prediction horizon T^+, for a given area $\phi \in \Phi$ and draw r, density which exceeds the congestion threshold:

$$\rho_{\phi,r}^{T^+} = \int^{T^+} \max(0, \rho(\phi, t)_r - \rho^c)dt. \tag{13}$$

The total congestion in all zones is the sum of the individual congestion in each zone:

$$\rho_{\Phi,r}^{T^+} = \sum_{\phi \in \Phi} \rho_{\phi,r}^{T^+}. \tag{14}$$

Finally, the average congestion in each zone for draw r is:

$$\overline{\rho_{\Phi,r}^{T^+}} = \frac{1}{|\Phi|} \rho_{\Phi,r}^{T^+} \tag{15}$$

We compute the mean across all draws to reduce the distribution to a scalar:

$$\overline{\rho_{\Phi}^{T^+}}(s) = \frac{1}{|R|} \sum_{r \in R} \overline{\rho_{\Phi,r}^{T^+}} \tag{16}$$

Equation (16) is the second metric monitored. The third metric we include in the multi-objective optimization algorithm is a measure of congestion variability across zones. We wish to measure the gap between the average congestion and the largest congestion observed in the areas Φ. We achieve this by computing the difference between the average congestion and the largest congestion:

$$\overline{\rho_{\Delta}^{T+}}(s) = \frac{1}{|R|} \sum_{r} \max_{\phi \in \Phi} \rho_{\phi,r}^{T+} - \overline{\rho_{\Phi,r}^{T+}}. \tag{17}$$

As for the average congestion in each zone, we compute the mean value across the different simulation draws. For the sake of notational simplicity, the explicit dependence on the control configuration s has been omitted in places. Nevertheless, the three indicators naturally depend on s.

Including three different objectives in the optimization problem requires adaptations to the minimization algorithm. Instead of using a linear combination of these three indicators which require the definition of weights, we propose an adaption of the ALNS algorithm which exploits the concept of a Pareto frontier. This approach not only circumvents the need for weights which are challenging to define, but also broadens the search since a collection of solutions are maintained. Instead of having one single solution to use for generating the next candidate, the algorithm now has a collection of solutions to use for generating candidates. From this collection of solutions, one must be selected and implemented during the next interval Δt_u. We suggest the selection of the control configuration which produced to lowest travel time measure. This choice emphasise travel time over congestion. The problem which is solved for the multi-objective predictive control algorithm is the following:

$$\begin{aligned} s_{opt} = \arg\min_{s} \quad & \overline{\chi^{\tau+}}(s), \overline{\rho_{\Phi}^{T+}}(s), \overline{\rho_{\Delta}^{T+}}(s) \\ \text{s.t.} \quad & s \in \mathcal{S} \end{aligned} \tag{18}$$

The operators used for this multi-objective ALNS are the same as those used for the single objective algorithm. Nevertheless, one new element is introduced: the neighbourhood size $\alpha \in [0, 1]$ is controlled by the algorithm, and not drawn randomly. The values of α are selected from a predefined list $\mathcal{A}$, sorted in increasing value. The neighbourhood size α is linked to the fate of the current solution. Each time a solution is added to the Pareto frontier, the value of α is set to the first value in $\mathcal{A}$. Then, for each iteration, α is set to the next value from $\mathcal{A}$, hence α will increase at each iteration until a new solution is inserted into the Pareto frontier. This procedure gradually increases the distance between the reference solution x^c and the generated solution x^{i+1}.

Algorithm 5: Multi-objective ALNS

Input:
feasible solution: x
operator set: Θ
Initialization:
operator weights: g
iteration counter: $i = 0$
maximum number iterations: n
reference solution: $x^c = x$
pareto set: $S = \{\}$
dominated set: $D = \{\}$
Iterations:
while $i < n$ **do**
    select operator o and neighbourhood size α
    update reference solution x^c
    generate new solution $x^{i+1} = o(x^c, \alpha)$
    evaluate $c(x^{i+1})$
    if $x^{i+1} \in S$ **then**
        solutions dominated by x^{i+1} : d
        $S = S \cup \{x^{i+1}\}$
        $S = S \setminus d$
        $D = D \cup d$
    else
        $D = D \cup \{x^{i+1}\}$
    end
    update g
    $i = i + 1$
end
Output: pareto optimal set S

In this section, we have proposed three variations of the control algorithm. The fixed algorithm exploits only historical data, the reactive algorithm using real-time data while the predictive algorithm which uses short-term predictions. The data used by the control algorithms is provided by a DPMS. The implementation detail and modelling assumptions made to build the simulation environment in which these algorithms are tested are presented in the beginning of the following section which presents the first case study.

5 Single corridor infrastructure

The three control algorithms we described in the previous section are tested in a simulation environment. By doing so, we can evaluate whether moving walkways are promising devices for controlling pedestrian flows and whether the predictive

control algorithms are better than the reactive algorithm. The first case study is a subset of a train station with one single corridor. The second setup is a more complex infrastructure with two corridors. After describing the infrastructure configuration of the first case study, we present the modelling decisions and DPMS implementation details.
The first case study we present is a subset of the train station in Lausanne, Switzerland. This is the same physical walkable space used in Molyneaux et al. (2019). A pedestrian tracking system was used in 2013 in the station to collect empirical data. This data set is used as the demand scenario for the simulations. We simulated the installation of moving walkways along the most busy pedestrian underpass of the station (Figure 4).
The three control algorithms described in section 4 are tested and their impacts are analysed with regard to pedestrian travel time and density. Four different sets of simulations have been performed. The first is the reference scenario without any moving walkway installed. This setup is used as the reference scenario for measuring the impact of the different moving walkway configurations. The second scenario is the use of moving walkways with a fixed control algorithm built upon historical data. The third scenario uses the reactive control algorithm. The fourth and final scenario uses the predictive control algorithm. These four scenarios are referred to as, in order, "no-mw", "fixed", "reactive" and "predictive". For all scenarios, 100 replications of the simulations are performed to build a distribution of the performance indicators. The time horizon is set to five minutes. A short time period (five minutes) was chosen such that the predictive control strategy can optimize the control configuration over the whole interval in one horizon.

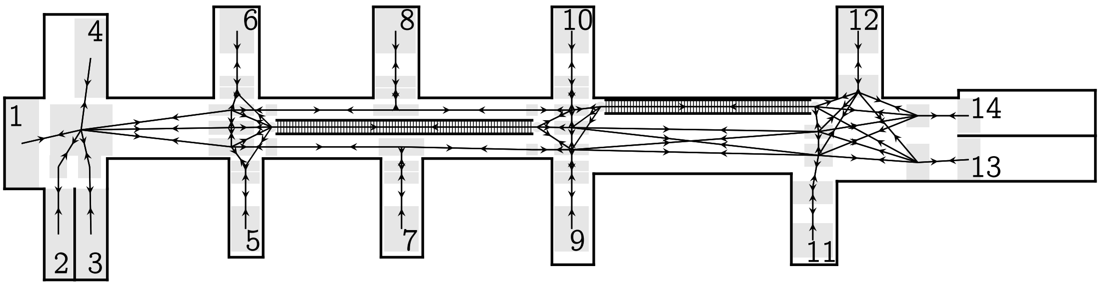

Figure 4: Single corridor infrastructure representation. MW-1 is on the left and MW-2 is on the left.

DPMS specification The components needed to implement a DPMS are detailed in Molyneaux et al. (2019), where definitions of spatial and temporal representations, supply, demand, fundamental quantities and data, control, state estimation and prediction and finally control configuration generation are provided. The first element we discuss is the spatial representation.
We use a bi-level approach for modelling the spatial environment, similarly to Molyneaux et al. (2019). The walkable floor space is modelled as a continuous

space in which pedestrians avoid obstacles and other pedestrians. This operational model is taken from the NOMAD package (Campanella, 2016). The tactical model relies on a graph which allows pedestrians to navigate the walkable space. We assume pedestrians have full knowledge of the congestion inside the infrastructure (Hoogendoorn and Bovy, 2004). This is modelled by updating each link travel time every time a pedestrian leaves the link. The tactical route choice decisions are modelled using the shortest path. All elements composing the infrastructure L are static except for the collection of moving walkways $\mathcal{W}$.
We model pedestrians individually, as in Molyneaux et al. (2019). The demand is modelled such that each pedestrian $n \in N$ has the following attributes: desired walking speed sampled from a normal distribution ($\mu = 1.34m/s$, truncated at $3.0m/s$), origin and destination zones and generation time. Pedestrians are generated at a disaggregate level according to either empirical observations or a Poisson process.
The computation of density used in this case study is based upon Voronoi tessellations. This method generates pedestrian-specific density values inside a defined area L'. Therefore, Voronoi tessellations generate a density distribution inside a given area. We compute the upper quartile (75% percentile) of this distribution to obtain a scalar value for density inside L' at time t:

$$\rho(L', t) = Q_3 \left[\rho_n(t) \;\; \forall n \in N_{L'}(t)\right], \tag{19}$$

where Q_3 represents the upper quartile, ρ_n the density associated with individual n and $N_{L'}(t)$ the pedestrians inside L' at time t. The utilization of Voronoi tessellations decreases the dependency on the arbitrary area in which density is computed (Nikolić et al., 2016). Since the individual density values show high variability over time, we use the upper quartile, instead of the maximum, to reduce the density distribution to a scalar. This reduces sudden jumps in the density computation over time. The density threshold above which we consider congestion takes place is set to $\rho^c = 1.08pax/m^2$. This threshold corresponds to the level-of-service E defined in Fruin (1971).
For the reactive control algorithm, the calibration of the controller gains is accomplished empirically according to the "trial-and-error" procedure described in Mulholland (2016). A sequence of steps to follow for estimating the regulator gains is provided. They rely on observing the process output after applying changes in the controller gains. The set point for PI controller is set to $\rho^s = 1.08pax/m^2$.
The predictive control algorithm uses the single-objective optimization algorithm. The short-term predictions are run with 150 iterations of the single-objective ALNS algorithm and 12 replications of each control configuration evaluation. In this paper, the short-term predictions are performed using the same simulator as the main simulations. This means the predictive algorithm has access to "perfect" information. Considering we design and test the moving walkways as a control strategy in a simulation environment, state estimation is not needed. The simu-

lator generates the required data.
Performing short-term predictions over the whole simulation period would not be feasible in practice. Nevertheless, this provides valuable insight regarding the capacity of the algorithm to improve the pedestrian dynamics. A rolling horizon scheme will likely not achieve the same performance, hence this solution can be considered an upper bound to the improvements we can expect from the predictive control algorithm. The utilization of the same simulator for the short-term predictions as for the main simulator is done for practical reasons. Firstly, it removes the need to implement a second pedestrian simulator. Secondly, there is no need for temporal synchronization and spatial aggregation/disaggregation between different models. Furthermore, we assume that the data collection process is perfect and complete, hence state estimation is not required. In practice, such assumptions cannot be made for multiple reasons. The main simulator replaces real-life dynamics, hence one single pedestrian simulator used for the short-term predictions is sufficient. Nevertheless, measurement devices are needed and generate data with errors and biases. Furthermore, collecting data covering the whole infrastructure can be costly, hence measurement devices cover only certain areas of the walkable space. With partial data coverage state estimation is needed, which induces uncertainty into the data. Therefore, even though the usage of perfect prediction information simplifies the problem at hand, investigating the different algorithms in such a simulation environment will produce valuable information regarding their effect on the pedestrian dynamics. The robustness of the control algorithms to measurement errors and the state estimation process is left for future work.
Next, we present the results from the different simulation scenarios and analyse the impact of the different control strategies on the pedestrian dynamics. We start by discussing aggregate indicators.

Aggregate indicators

We start by discussing the effect of the different control strategies on aggregate indicators. Figure 5 shows boxplots for different aggregate indicators: mean travel time (eq. 11) and congestion, based on eq. (16). One small alteration has been made to eq (16). Instead of considering the mean congestion per zone, we consider the total congestion in all zones. The mean travel time box plots (Figure 5a) show the advantage of control algorithms which dynamically update the configuration based on the measured KPI. The mean travel time decreases by approximately 9% when such control strategies are used. Secondly, the "fixed" control strategy is poor at decreasing travel time compared to the "no-mw" scenario. The density box plots (Figure 5b) show that the congestion experienced by pedestrians in the corridor junctions is lower for dynamically controlled moving walkways. We expected the "reactive" and "predictive" algorithms to improve travel time and

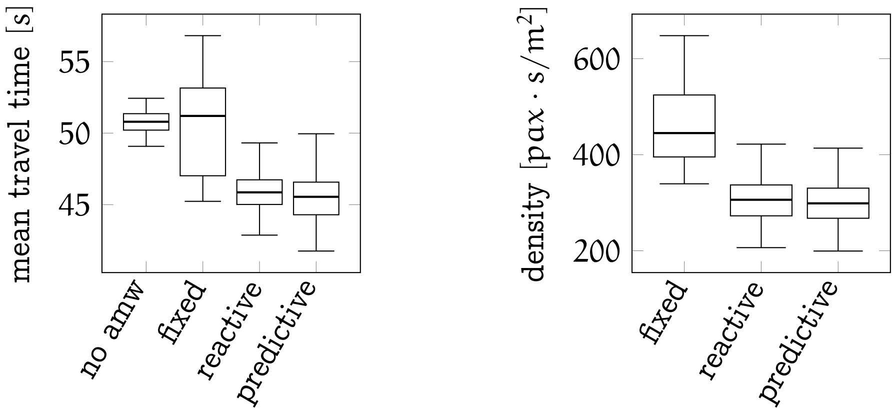

(a) Mean travel time. (b) Integral of congestion.

Figure 5: Box plots of aggregate performance indicators for the different scenarios.

density compared to the "fixed" algorithm since they adapt to the demand (unlike the "fixed" algorithm). Congestion is measured in each corridor intersection and at both extremities of each moving walkway since these control devices tend to attract pedestrians at their ends and create congestion. The difference between the "reactive" and "predictive" strategies is negligible in terms of both travel time and density. Since the moving walkways concentrate congestion in the intersections, comparing the congestion in the intersections between the "no-amw" algorithm and the control algorithms is not meaningful.

OD specific travel times

As shown previously, the dynamic control algorithms successfully improve travel time but no difference between the "reactive" and "predictive" flavours has been observed. Therefore, we discuss the impact of theses strategies at an origin/destination level. Figure 6 presents the change in relative travel time for all origin and destination pairs. The Welsch T-Test (unequal variance and unequal sample size) is used to test the null hypothesis that the mean travel times per origin/destination are equal. The test is performed between the reference scenario and a given control algorithm. The OD pairs are sorted based on the category of trip they represent (Figure 6d). The different categories are based on the usage of moving walkways and the length of the "walking legs". Group A represents passengers changing platform but don't have any MW along their path, for example walking from zone 5 to zone 7 (Figure 4). Group B includes trips where one MW can be used and no walking legs are required (zone 5 to 9 for example). Group C covers trips with one MW and a walking leg (zone 1 to 9). Category D covers all trips with two MW on their path. Finally, E covers the other OD trips (zone 11 to 14 for example). Figure 6a shows, for each OD pair, the relative change in travel time between the reference scenario and the fixed control algorithm. Each dot is one OD pair. The type of dot depends on the confidence one can give to its value. Black circles mean that at least five pedestrians have used it per replication and that the value is statistically significantly different from 0 (equal mean hypothesis). Grey circles indicate that at least five people have used the OD, but the T-Test does not reject the null hypothesis. Black crosses are OD pairs where less than five people have used this OD pair (on average), and the null hypothesis is rejected. Finally, grey crosses indicate that less than five people have used the OD pair and the null hypothesis cannot be rejected. Figures 6b and 6c show the results for the reactive and predictive control algorithms.

The "fixed" control algorithm decreases but also increases travel times for many OD pairs. This is expected as the direction and speed of the walkways does not change based on the occurring pedestrian dynamics. Therefore, the walkways will not slow down if downstream congestion occurs, neither will they change direction if the majority of pedestrians are moving in the other direction. OD pairs which use one moving walkway sometimes benefit and are sometimes penalized by this control algorithm (groups B and C). Most of the OD pairs from groups B and C which are penalized by the walkways are those involving zones 7 and 8. The explanation is found by considering the position of the left moving walkway. Since it's installed in the middle of the corridor, two narrow corridors are created either side of it. This separation reduces the space available for the pedestrians walking to/from zones 7 and 8. This situation is therefore more prone to congestion under high demand. OD pairs which allow the usage of both moving walkways generally benefit from the installation of moving walkways on the other hand.

The analysis of Figure 6b reveals the advantage of dynamically controlled moving walkways: fewer OD pairs suffer from an increased travel time and the amplitude of these negatively affected ODs is small. The pedestrians who suffer from the moving walkways are found in the same group as those suffering from the "fixed" control algorithm. Furthermore, they are also those entering or exiting the simulation through zones 7 and 8. Finally, the overall changes in travel time are more compact compared to the "fixed" algorithm, hence the change in travel time is more consistent across OD pairs.

The predictive control algorithm further improves the overall travel times per OD. The number of OD pairs which suffer from this control algorithm are further reduced compared to the reactive algorithm (sub-figure 6c). The pedestrians which are negatively (statistically) significantly impacted are those moving from zone 8 to zones 13 and 14. The explanation provided before regarding the width of the available corridor explains this increase. Pedestrians using two moving walkways (group D) clearly benefit from the strategy, like with the reactive algorithm. The second major difference between the predictive and reactive algorithms lies in the consistency across OD pairs. The reductions in travel times are slightly smaller than those with the reactive algorithm, but few OD pairs suffer from an increased travel time. Hence the predictive algorithm is a scenario which can be considered

fairer between pedestrians.
Finally, we should mention that pedestrians who don't use any moving walkway (group E) are not significantly impacted by the algorithm choice. The majority of the change in travel times are not statistically significantly different from the reference scenario.

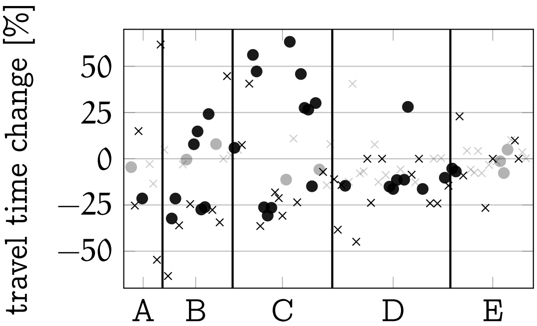

(a) no-mw VS fixed

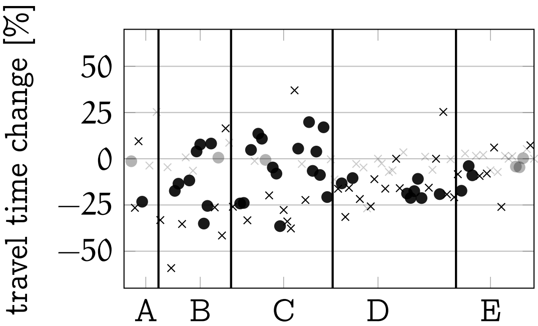

(b) no-mw VS reactive

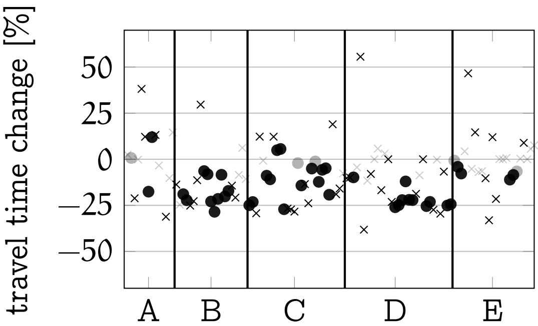

(c) no-mw VS predictive

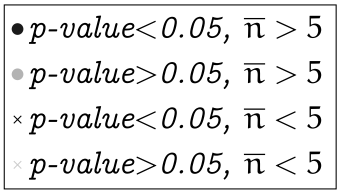

Label	Description	origin/destination IDs
A	Neighbouring platform without moving walkway	5-6 ↔ 7-8 & 7-8 ↔ 9-10
B	Single moving walkway without walking leg	5-6 ↔ 9-10 & 9-10 ↔ 11-14
C	Single moving walkway and walking leg	1-4 ↔ 9-10 & 7-8 ↔ 11-14
D	Two moving walkways	1-6 ↔ 11-14
E	Other	

(d) Origin-destination categorisation

Figure 6: Relative travel time comparison between the three moving walkway control algorithms and the reference scenario without moving walkways.

Average moving walkway speeds and pedestrian density

Understanding and explaining the different impacts of the reactive and predictive control algorithms requires in-depth analysis of the moving walkway speed profiles and density measurements. Figure 7 presents the average speed profile of the three control scenarios. The dotted line represents the speed profile for the "fixed" algorithm computed from historical data, hence it is the same for all replications. Two bands, one for the reactive algorithm and one for the predictive algorithm, represent the interquartile range of the MW speed based on the 100 replications of the simulation scenario. The band with solid lines concerns the predictive algorithm, while the band with the dashed line represents the MW speeds for the reactive scenario.

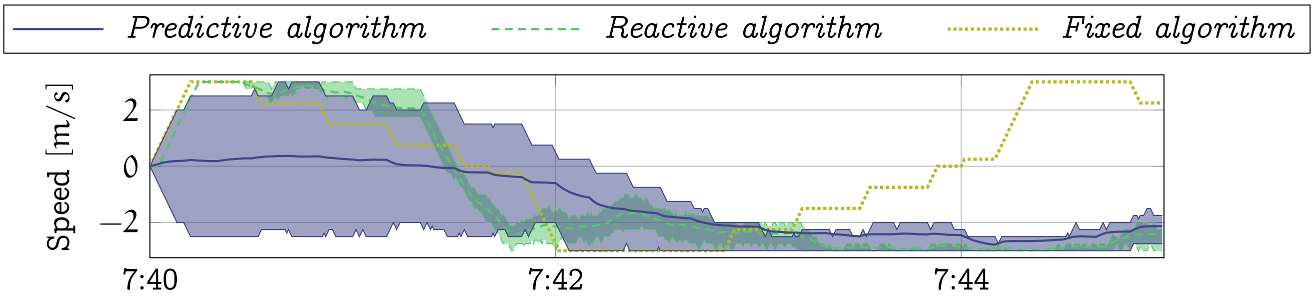

(a) Left moving walkway (MW-1)

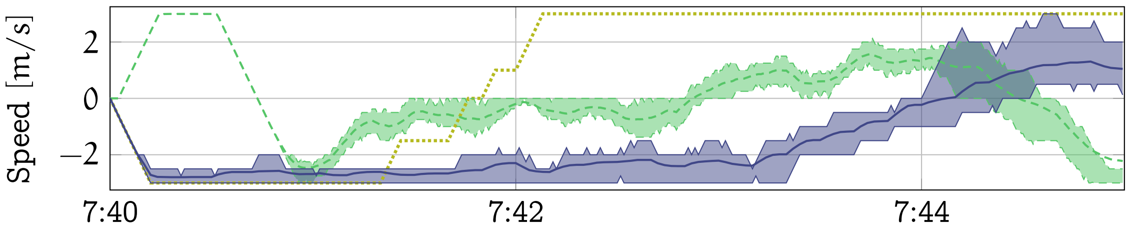

(b) Right moving walkway (MW-2)

Figure 7: Moving walkway average speed profile for the three different control algorithm scenarios.

The first observation we can make concerns the consistency of the "reactive" speed profile over the first 60 seconds of the simulation for MW-2 and over the first 100 seconds for MW-1. This is the case as the density measured inside the junctions is low for those time periods. When considering the density profiles from Figure 8, we see that little congestion occurs before 7:41, this for all zones. Therefore, the "reactive" moving walkways are always at maximum speed until congestion builds up. This changes as soon as congestion appears in the junctions. The "reactive" MW-2 slows down from 7:41 since congestion builds up in "junction 9-10".
On the other hand, the large variance in moving walkway configuration for the "predictive" version of MW-1 should be explained. We see that for the first minute of the simulation period, no congestion occurs at either end of this moving walkway (8b and 8c). Secondly, we also see that the pedestrian flows parallel to MW-1 are low and approximately equal. The combination of these two observations indicate that the predictive algorithm can choose either direction at high speeds as an optimal solution, which explains the large variance in speed profiles.

Later in the simulation, from 7:42, for both dynamic algorithms, MW-1 tends to operate close to the maximum speed moving pedestrians from junction 9-10 towards junction 5-6 (i.e. backwards, hence the negative speed). This direction is consistent with the pedestrian flows parallel to MW-1 shown in Figure 9. The flow moving in the negative direction of MW-1 is larger over all the time period of interest than the flow moving in the positive direction. Furthermore, the density in junction 9-10 is larger than that in junction 5-6 over all the time period, hence confirming that moving pedestrians away from junction 9-10 makes sense.

The direction of MW-2 over the first 150 seconds of the simulation can be explained using the flows from Figure 9 as well. The flow moving in the negative direction of MW-2 is larger than the flow moving in the positive direction. Nevertheless, the amplitude of the speed of the "reactive" MW-2 is significantly lower than that of the "predictive" MW-2. The density measured in junction 9-10 (sub-figure 8b) explains the decreased speed of the "reactive" MW-2. Since the density is above the target value of $1.08 pax/m^2$, the reactive algorithm will reduce the speed of the moving walkway to prevent downstream congestion.

The difference in pedestrian density during high demand (around 7:42) is different for both dynamic algorithms. The density in junction 9-10 is lower for the reactive algorithm compared to the predictive algorithm (8a). The opposite is observed in junction 11-12-13-14. There, the density is lower for the predictive algorithm (8b). The density levels are similar in both junctions for the predictive algorithm. This conclusion is similar to the previous conclusion about the travel times. The predictive control algorithm is fairer across users.

An unexpected peak in pedestrian density occurs, in junction 11-12-13-14, for the "predictive" algorithm around 7:44. The pedestrian density reaches a plateau higher with the predictive algorithm than it does for the other control algorithms. This small congested period occurs at the same time that MW-2 changes direction (Figure 7b) at 7:44. During a change in direction, the moving walkway must close for a short period of time. Furthermore, we see a small peak in the demand curve corresponding to the negative direction of MW-2. The congestion is therefore induced by this peak in demand and the closed moving walkways. The "fixed" and "reactive" algorithms, on average, are open during this small peak hence congestion does not occur.

Detailed MW-2 analysis

Figure 10 shows the speed profile of the "reactive" MW-2 and the density measurements in both junctions at either end of the moving walkway. This is a classic example showing the limitations of the reactive algorithm. From 7:41 to 7:43, the moving walkway is transporting pedestrians from junction 11-12-13-14 to junction 9-10 (negative speed). As soon as the density exceeds the congestion threshold ($1.08 pax/m^2$), the reactive controller reduces the speed of MW-2 to prevent exces-

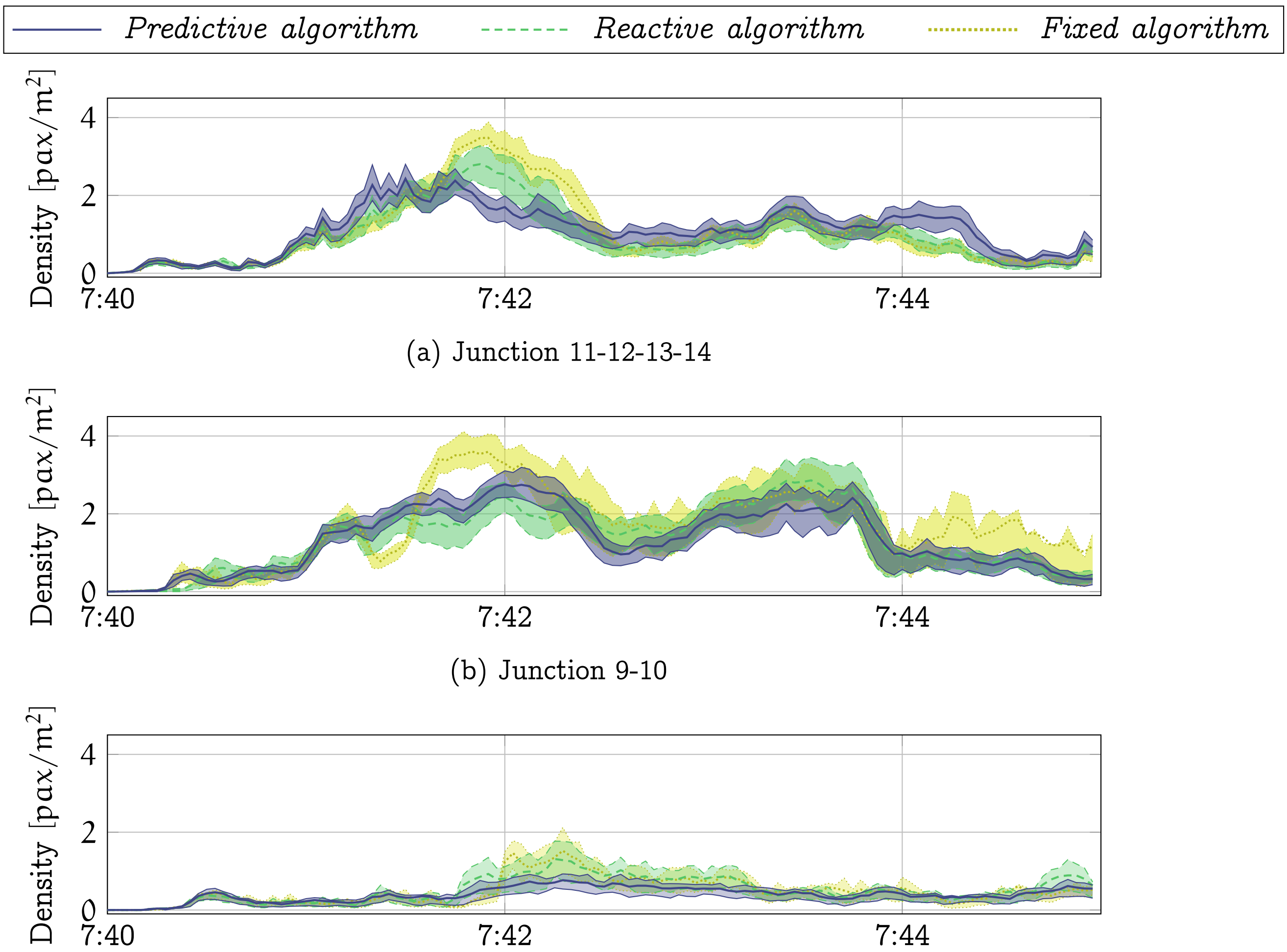

(a) Junction 11-12-13-14

(b) Junction 9-10

(c) Junction 5-6

Figure 8: Density evolution over time for all four junctions.

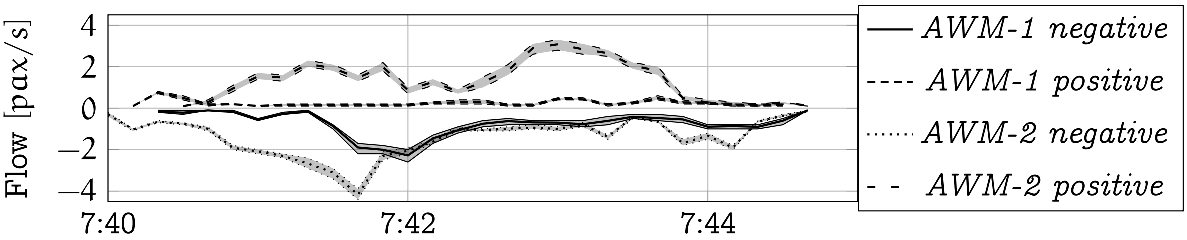

Figure 9: Pedestrian flow along the main corridors parallel to the moving walkways computed from the reference scenario "no-mw". A negative flow corresponds to pedestrians walking in the same direction as a moving walkway with negative speed.

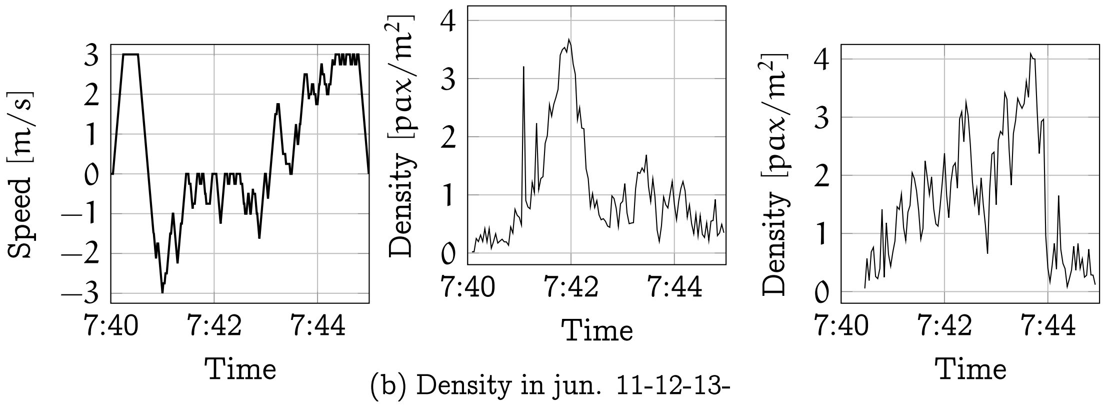

(a) Speed profile for MW-2

(b) Density in jun. 11-12-13-14.

(c) Density in jun. 9-10.

Figure 10: Speed profile and density measurements for a single realisation of the reactive control algorithm.

sive congestion. The oscillating effects of the MW-2 speed are visible in Figure 10a, and the corresponding oscillations can be observed in Figure 10c. Meanwhile, the density inside junction 11-12-13-14 is increasing which implies that MW-2 should accelerate to empty this junction. Therefore, a trade-off between the density levels in both junctions should be made. The predictive strategy is capable of addressing this trade-off since it monitors pedestrian travel time in the whole infrastructure and is capable of anticipating pedestrian demand.

Through this first case study we have shown that the dynamic strategies are significantly better than a fixed precomputed control configuration. Nevertheless, the "predictive" algorithm presents only little benefit over the "reactive" algorithm. Therefore, the added value of the short-term predictions is not obvious at this point. The next section presents a second, more complex case study.

6 Double corridor infrastructure

The previous case study highlighted the advantage of dynamic control strategies, but the short-term predictions did not provide a substantial benefit. To understand whether a predictive control algorithm for controlling moving walkways can positively impact pedestrian dynamics in a larger environment, we have analysed a more complex infrastructure. The walkable space is a simplification of the whole station of Lausanne, Switzerland. We have two corridors linking three platforms. A representation of the infrastructure is found in Figure 11. We simulate pedestrian movements along the platforms since individuals can walk along the platforms and choose which corridor to use. Four moving walkways are used in this infrastructure, two in each corridor. Route choice now becomes significant as pedestrians can change corridors to reach their destination. The time period of interest is 15 minutes long.

We use the same simulation environment as described at the beginning of the previous section, except for the tactical route choice model. Route choice is modelled using the path-size logit model (Prato, 2009; Ben-Akiva and Bierlaire, 2003). The parameters are taken from Liu et al. (2020b). The route is updated each time a pedestrian reaches a vertex in the graph. Given the poor benefits of the "fixed" control algorithm for the previous case study, we do not use this algorithm in this case study. We keep both dynamic control algorithms. The "reactive" algorithm is the same as previously presented. The "predictive" algorithm is applied in a true rolling horizon approach this time since we work on a longer time period. Furthermore, we use the multi-objective predictive control algorithm. The reference scenario and reactive control algorithm simulations were replicated at least 100 times. The predictive simulation was replicated twelve times due to computational time. The short-term prediction horizon is 3 minutes long and is updated every 1.5 minutes. 150 iterations of the multi-objective ALNS were performed at each prediction update, with 32 replications of the objective function at each iteration. We recall that the multi-objective control algorithms returns the Pareto optimal set of solutions, hence one particular solution must be selected from this set. The control configuration which is applied for the horizon is the one with the lowest travel time.

By monitoring congestion alongside travel time, we gain further insight into the trade-off taking place between the different metrics. The previous case study showed that the reactive and predictive algorithms had similar effects on pedestrian dynamics. Therefore, by explicitly including congestion into the optimization algorithm, and not only analysing it a posteriori, we emphasize how the different algorithms impact pedestrian flows. Another reason for explicitly monitoring the spread in congestion in the different intersections (eq. 17) is to prevent a significant unbalance in congestion throughout the walkable environment.

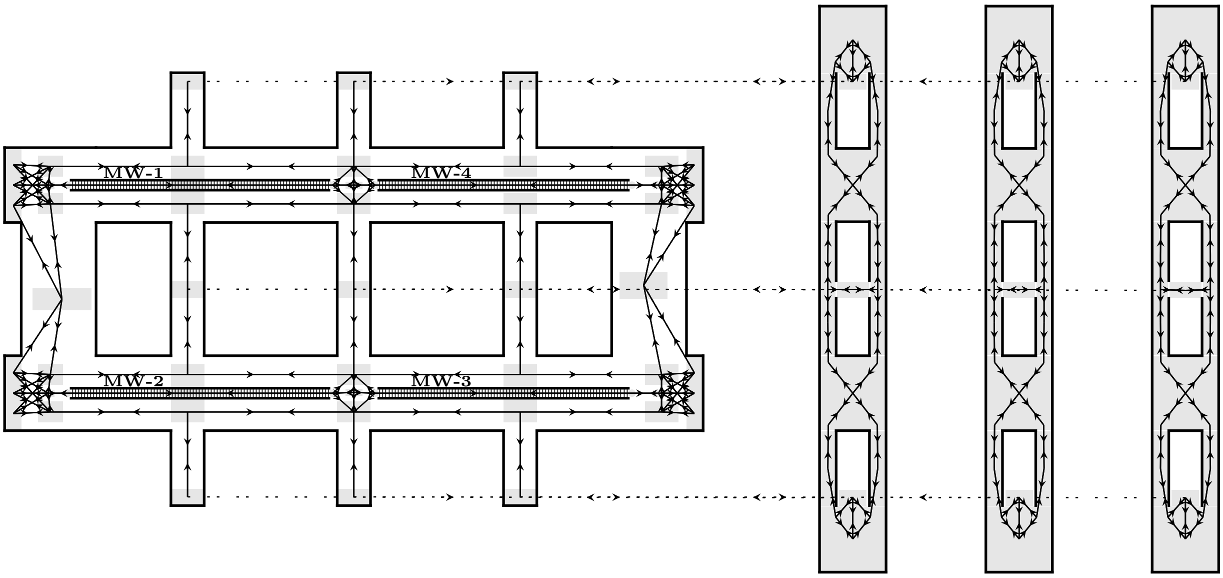

Figure 11: Three platforms infrastructure representation. The moving walkways are numbered counter clockwise: MW-1 top left, MW-2 bottom left, MW-3 bottom right, MW-4 top right.

Aggregate indicators

The aggregate travel time and congestion data plotted in Figure 12 tells a different story than the previous case study. Here, the predictive control algorithm is significantly better than the reactive algorithm. The mean travel time is reduced by approximately 25%. The congestion experienced by pedestrians at the extremities of the moving walkways is also lower for the predictive control algorithm. The reactive algorithm only improves the travel time by 5%. In the following paragraphs we will discuss the results in more detail to understand why the predictive and reactive algorithms induce different results for this case study.

OD specific travel times

The OD specific travel times are presented in Figure 13. Similarly to Figure 6, we present the OD specific relative change in travel time. The categorisation is different though. Three main groups are used based upon the number of MW along the route between the origin and destination. The second group (one MW) is split into two subgroups: towards platforms (B1) and leaving platforms (B2).
The reactive algorithm decreases but also increases travel time for many OD pairs. The group of ODs which do not use any moving walkway show a large dispersion in relative travel time change. No clear pattern stands out concerning the direction of pedestrian flow for these OD pairs. The travel times of pedestrians who could use one moving walkway can be slit into two groups: those moving from platforms towards the main corridors, and those moving from the corridors towards the platforms. On one hand, when pedestrians move to platforms (group B1), they are

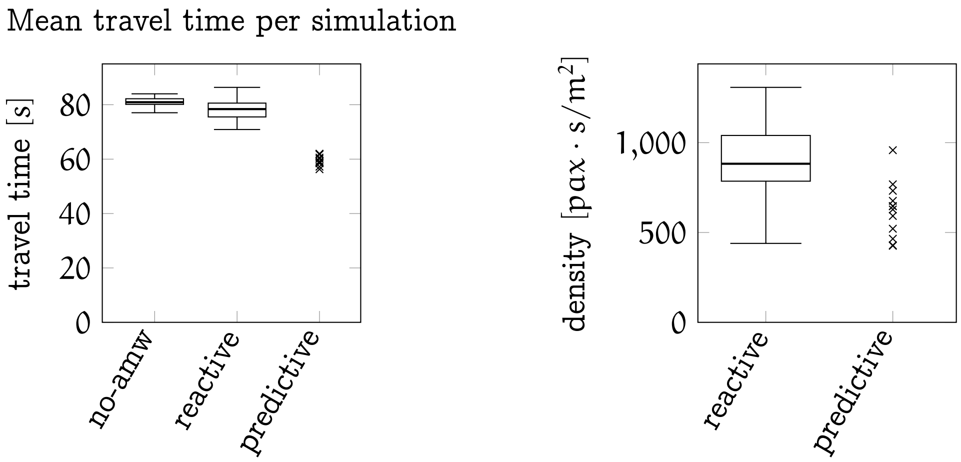

(a) Mean travel time. (b) Integral of congestion.

Figure 12: Box plots of aggregate performance indicators for the different scenarios.

generally penalized by the reactive control algorithm. Three ODs pairs do not follow this rule (the three black circles below zero in group B1). On the other hand, when pedestrians move from the platforms into the corridors (group B2) they all benefit from the reactive algorithm. The groups of pedestrians which have two moving walkways along their path all benefit from the reactive algorithm.
The predictive algorithm boasts more consistent results in terms of travel times. Except for one OD pair, all statistically significant differences are improvements. Furthermore, all OD pairs with moving walkways along their paths benefit from the control algorithm. Another difference is visible when comparing the amplitude of the improvements between both graphs: the predictive algorithm shows larger improvements than the reactive algorithm. This observation is the opposite compared to the previous case study (Figure 6). Finally, the pedestrians which can use one moving walkway and are walking towards the platforms are those who benefit the most in terms of travel time. This is the opposite to the reactive algorithm. In general, the predictive algorithm is fairer across ODs than the reactive algorithm since nearly all ODs pair benefit from the control strategy.

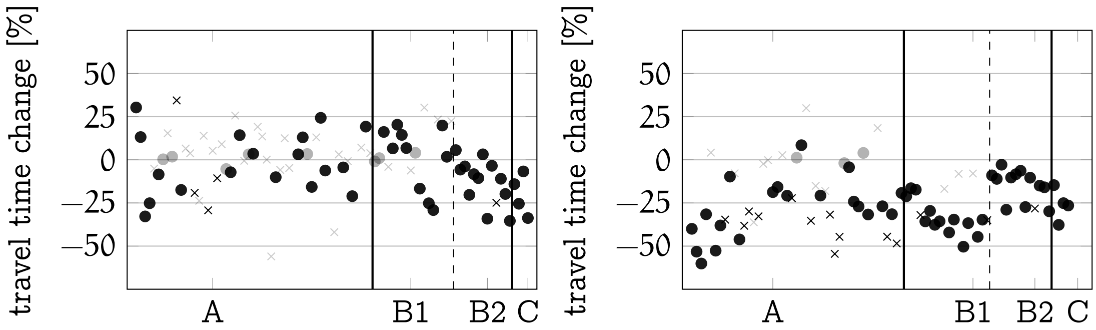

(a) no-AMW VS reactive

(b) no-AMW VS predictive

Label	**Description**
A	no MWs along path
B1	one MW along path, to platforms
B2	one MW along path, from platforms
C	two MW along path

● *p-value*$<$*0.05*, $\overline{n} > 5$
● *p-value*$>$*0.05*, $\overline{n} > 5$
× *p-value*$<$*0.05*, $\overline{n} < 5$
× *p-value*$>$*0.05*, $\overline{n} < 5$

Figure 13: Relative travel time change for the reactive and predictive algorithms compared to the reference scenario without moving walkways.

Pedestrian walking speed

The mean pedestrian walking speed computed over time is presented in Figure 14. The pedestrians have been grouped into intervals based on their entry time into the system. Both dynamic control algorithms improve the pedestrian walking speed compared to the reference scenario. Nevertheless, no clear advantage of one dynamic algorithm over the other is apparent. The walking speed decreases as demand increases. This is clearly visible between 7:41 and 7:42 where many pedestrians enter the system. During this high demand period the walking speed decreases due to congestion inside the infrastructure.

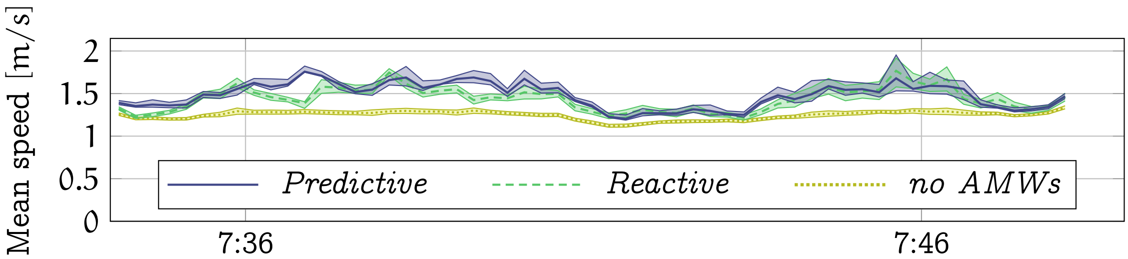

(a) Mean walking speed over time.

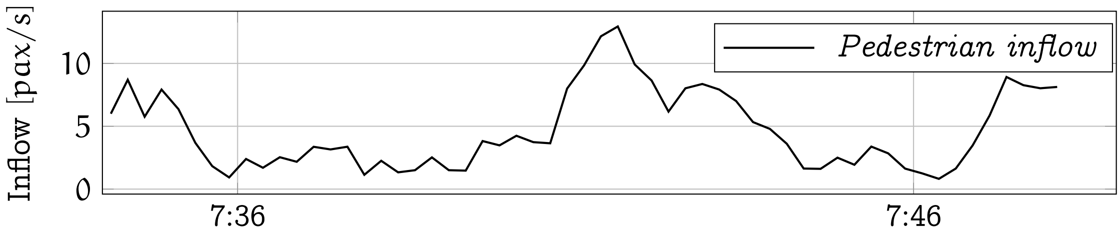

(b) Inflow into the infrastructure over time.

Figure 14: Pedestrian walking speed and pedestrian inflow into the infrastructure over time.

Moving walkway speed and pedestrian dynamics

The moving walkway speed profiles, pedestrian density at both extremities and parallel flows for all four moving walkways are presented in Figures 15, 16, 17 and 18. In the following paragraphs, we discuss how the reactive and predictive control algorithms influence the pedestrian densities.

The reactive algorithms behave similarly for MW-1 and MW-2. During most of the simulation period they operate at maximum speed, moving pedestrians from their "end" to their "start" (negative speed). Few pedestrians are using this sub-route (Figures 15b and 16b) and the density is higher at their "end" areas. Therefore the reactive algorithm is moving pedestrians from the high density area to the low density area.

The predictive algorithms behave differently than the reactive algorithms. MW-1 shows positive speeds for the first half of the time period (until 7:41), then a shift towards negative speeds happens. Nevertheless a large variance in speeds is visible. Similarly to the reactive algorithm, congestion vary rarely takes place (Figure 15c). The consistent positive speeds is a consequence of the absence of congestion and the slightly larger pedestrian flow moving in the positive direction. Since the predictive strategy minimizes travel time, the larger pedestrian flow contributes more to the mean travel time decrease than the smaller flow. Concerning the predictive MW-2, a large variation is observed in the speed profile except around 7:41 and for the last 2 minutes of the simulation. MW-2 moves people in the negative direction just after 7:41 to decrease density. The predictive algorithm successfully prevents congestion taking place at 7:42, which the reactive algorithm does not. During the last few minutes of the simulation, MW-2 systematically moves pedestrians from the "end" to the "start" to decrease density. Although the reactive MW-2 is moving in the same direction, the density is larger for the reactive algorithm, hence the explanation for this must be found elsewhere.

The speed profile for MW-3 differs significantly for the reactive and predictive algorithms. We first discuss the predictive algorithm, in light of the density at the "end" zone of MW-2, which is also the "start" zone of MW-3. We previously saw that the pedestrian density is significantly higher for the reactive control algorithm near 7:48. In Figure 17a, near 7:48, we see that the reactive and predictive algorithms have different behaviours. The reactive algorithm produces positive speeds, while the predictive algorithm produces negative speeds. The reactive algorithm behaves "as expected" since it moves people away from the high density at the "start". The predictive algorithm, on the other hand, is moving pedestrians into the higher density area but at reduced speed. By forcing the pedestrians moving in the positive direction to walk, the predictive algorithm spreads the demand in space, hence exploiting the full walkable space. This prevents congestion building up at the exit of the moving walkway, which is what happens for the reactive algorithm. The pedestrians moving in the opposite direction can use the moving

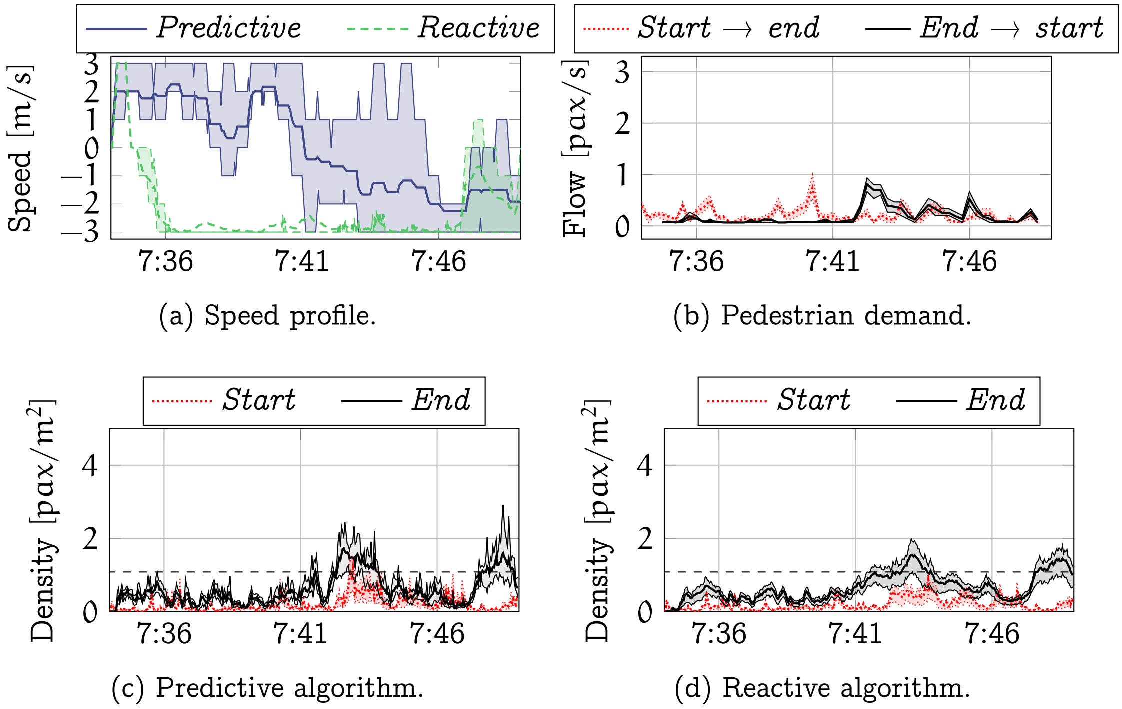

(a) Speed profile.

(b) Pedestrian demand.

(c) Predictive algorithm.

(d) Reactive algorithm.

Figure 15: Speed, density and flow data for MW-1.

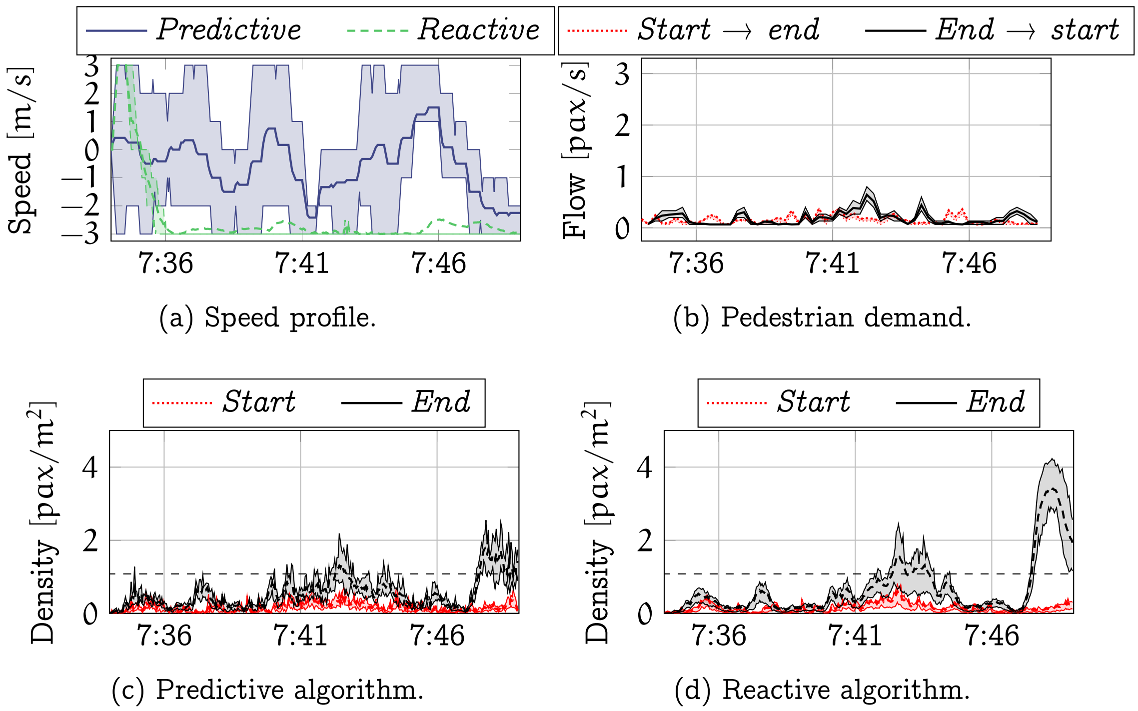

(a) Speed profile.

(b) Pedestrian demand.

(c) Predictive algorithm.

(d) Reactive algorithm.

Figure 16: Speed, density and flow data for MW-2.

walkway. This counter intuitive result shows the added value of an optimization-based predictive algorithm.
The fourth and last moving walkway emphasizes the “slower is faster” effect. During the peak in demand around 7:43, the reactive algorithm consistently reduced the speed of MW-4 to prevent congestion building up in the “start” area. Strong congestion takes place at the “end” and the moving walkway is moving the pedestrians away from this area (negative speed). Nevertheless, congestion also starts to build at the other end, hence the speed reduces to prevent congestion. The predictive algorithm behaves in a similar way. MW-4 operates at high negative speed to move the pedestrians away from the congestion during the first few minutes of the time period. This is confirmed by the negative pedestrian flow in Figure 18b. Then, from 7:41 the moving walkways consistently reduce their speed to low speeds, sometimes even closing it. By doing so, pedestrians must walk along both sides of the moving walkway and don’t aggregate near the entrance of the moving walkway. By reducing the moving speed of pedestrians, the predictive algorithm is able to spread the congestion in time and space.

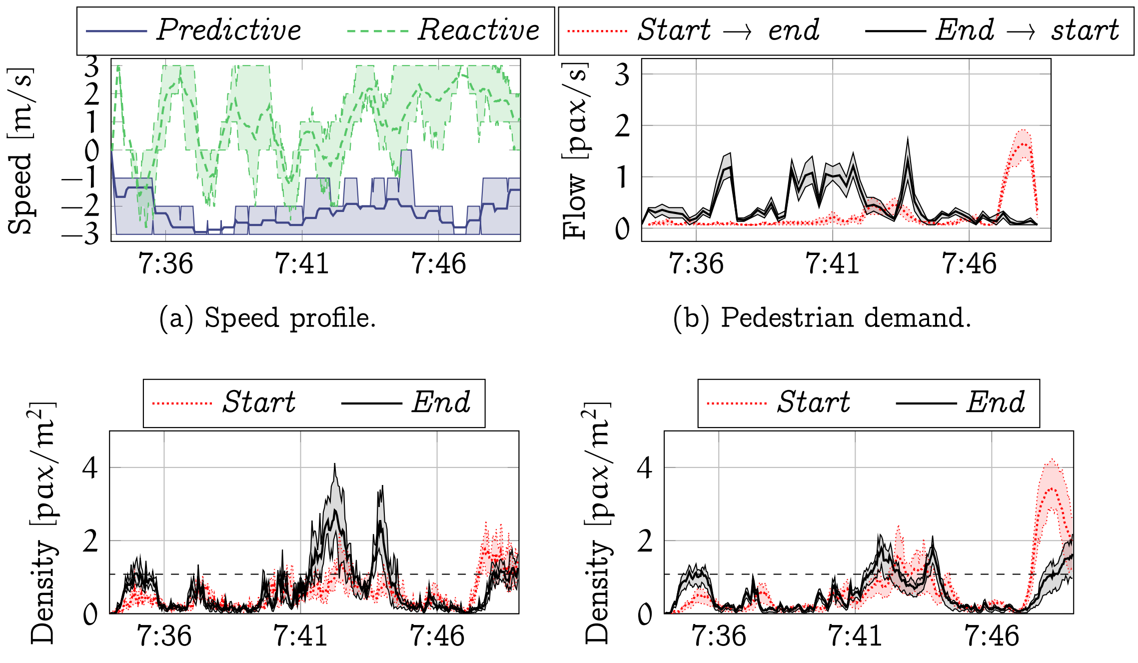

(a) Speed profile.

(b) Pedestrian demand.

(c) Predictive algorithm.

(d) Reactive algorithm.

Figure 17: Speed, density and flow data for MW-3.

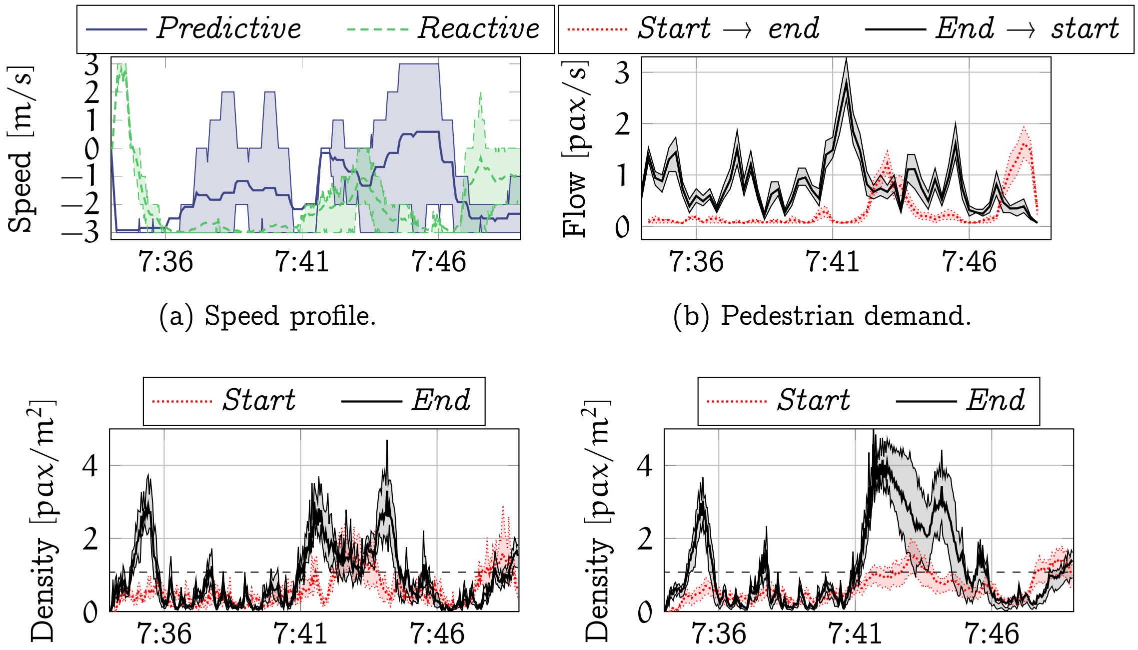

(a) Speed profile.

(b) Pedestrian demand.

(c) Predictive algorithm.

(d) Reactive algorithm.

Figure 18: Speed, density and flow data for MW-4.

Through the analysis of the behaviour of the reactive and predictive control algorithms in this second case study, we showed in which situations the predictive algorithm can reduce pedestrian congestion inside the infrastructure. We have seen that the predictive algorithm can generate solutions which are significantly different from the ones generated by the reactive algorithm. The predictive algorithm makes large pedestrian flows walk to prevent excessive congestion in the junctions. By doing so, the predictive algorithm balances travel time and congestion.

Pareto frontier analysis

The predictive algorithm relies on solving the optimization problem where the moving walkway speeds are the decision variables, and the objective function is a collection of indicators which summarize the pedestrian dynamics. The following paragraphs discuss the results from multi-objective ALNS algorithm presented in section 3 for two cases: low and high pedestrian demand. We recall that the predictive algorithm for this second case study relies on a multi-objective Pareto front optimization. We recall the three objectives which are used mean travel time $\overline{\chi^{T+}}$ (eq. 11), mean congestion $\overline{\rho_{\Phi}^{T+}}$ (eq 16) and congestion variability $\overline{\rho_{\Delta}^{T+}}$ (eq. 17). Furthermore, we recall that during one optimization horizon, the moving walkway speeds are split into intervals of 30 seconds.

Low demand Figure 19 contains the pareto front for the three variables and the visualization of the control configurations for each point on the pareto front for a prediction horizon with low density (7:37 - 7:40). The first conclusion we can make concerns the strong correlation between two indicators: $\overline{\rho_{\Phi}^{T+}}$ and $\overline{\rho_{\Delta}^{T+}}$ (Figure 19c). This is also visible in the pareto front comparing travel time to both measures of density (Figures 19a and 19b) where the Pareto fronts are nearly identical. Therefore, one of the density indicators is redundant for low density scenarios.

The control configurations for each point on the Pareto front provide us with insight into the trade-off between travel time and density which must be made. This is most visible in Figure 19g (MW-3) where the three solutions with the highest mean travel time stand out from the other solutions. On one hand these solutions present the lowest congestion, but on the other they present the highest travel time. The control configurations for these three solutions are different from the rest of the solutions. Most of the solutions have speeds between -2 and -3 during the whole optimization procedure, whereas for these three solutions which stand out their speeds are either positive or changing direction during the horizon.

The differences in objective function values can be explained when considering the pedestrian demand in the corridor where MW-3 is installed. The pedestrian flow in the negative direction along the corridor where MW-3 is installed is significantly larger the demand in the positive direction (Figure 17b). Therefore, two situations appear. In the first case, most of the solutions are moving the larger group of pedestrians with a higher speed thanks to the moving walkway, hence the lower travel time but creating some congestion in the process. For the second case, the three solutions with lower density but higher travel time are moving the smaller group of pedestrians, hence having less impact on travel time, but also preventing congestion from appearing.

One other solution stands out in these other graphs as well: the solution with the lowest travel time. This solution is particularly visible in 19e. A similar analysis can be made as with the three high travel time solutions. The pedestrian demand

parallel to MW-4 is larger in the negative direction than the positive one. This particular solution is favouring travel time over density since this solution also boasts the highest density values.
These two examples of different categories of solutions, hence of control configurations, emphasize the added value of considering a multi-objective approach when searching optimal control configurations. Since the set of pareto-optimal solutions contains the trade-off, the control strategy has the potential to give priority to different aspects of the pedestrian dynamics.

High demand The results for the high demand prediction are presented in Figure 20. The correlation we observed between both density indicators is not as clear in this context. On one hand, when one density indicator is low, so is the second one. On the other hand, when the mean density increases, the variance in $\overline{\rho_\Delta^{\tau^+}}$ (17) becomes large. Therefore, if the objective is to minimize density, then one density indicator is sufficient. But when a trade-off is explored between density and travel time, both density metrics are needed to distinguish the solutions. The lowest values of travel time are found with intermediate values of congestion (dark points in Figure 20c), again emphasizing the need to carefully study the trade-off between congestion and travel time.
For MW-3 (20g), we see that two solutions are identical (the two dark lines). The speed is -3 for the whole interval for these solutions. This gives us insight into the variance of the system. They are very close in terms of travel time and average density, but the $\rho_\Delta^{\tau^+}$ indicator differs for both solutions.
The solutions on the pareto front can be grouped into three categories based upon the three indicators: high travel time and low density (light lines), low travel time and high density (dark lines), intermediate travel time and density (intermediate lines). These three groups can be found in the control configurations of MW-1 (20d) and MW-3 (20g). For MW-2 and MW-4 these groups are not visible (20f and 20e).
We can distinguish the three groups when considering the speeds in MW-3 (20g). The group with high travel time (light lines) contains speeds which peak to $+3m/s$ for the third decision variable while the other decision variables are close to 0 or -1. The group with intermediate travel time and density values are solutions where the speed is generally between 0 and $-1m/s$. The two solutions with low travel time and high density have speeds fixed to $-3m/s$. Similarly, when considering the speeds profiles for MW-1 (20d), we can also distinguish the three groups of solutions. These three groups of control configurations show that different speed profiles will give priority to different objectives (travel time or density).
On the other hand, when looking at the control configurations for MW-2 and MW-4, the speed profiles do not allow us to differentiate the three groups of solutions. They operate between $+1m/s$ and $-1m/s$ in general. We can therefore conclude that the pareto front is governed by MW-1 and MW-3 since for the other two

walkways the indicators are not directly affected by the different control configurations.
A final remark concerning the variance of the indicators with respect to the control configuration consistency must be made. In Figures 19g and 20e the control configurations are generally consistent with each other although the indicators vary. This phenomenon has two potential origins: simulation-based stochastic variation and exogenous influence. Identifying the cause of the variation is challenging since both causes impact the same metrics. Considering the fact that changes in moving walkway speed between $-3m/s$ and $-2m/s$ have a very small impact on the indicators the discretization of the walking speeds can certainly be made less fine without loosing the advantages of a predictive control algorithm. Longer intervals would also simplify the optimization procedure and make the results more robust to stochastic variations.

By analysing the solutions on the pareto front for two different demand contexts, we have emphasized the added value of a multi-objective optimization framework for predictive control configuration generation. Even when demand is low, different control configurations can impact the overall travel time of the pedestrians. This effect is emphasized for high demand cases. Different control configurations will lead to different dynamics where travel time or congestion are low. Furthermore, not all control devices have the same impact on the system. Some moving walkways significantly impact the indicators while others only have minimal impact.

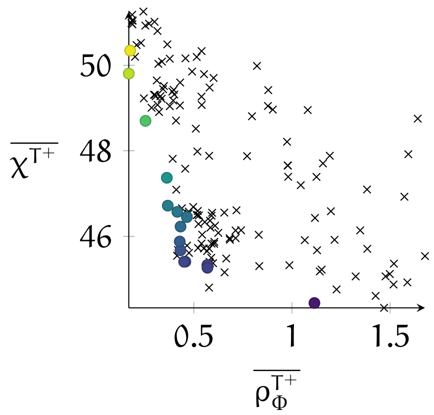

(a) density VS travel time

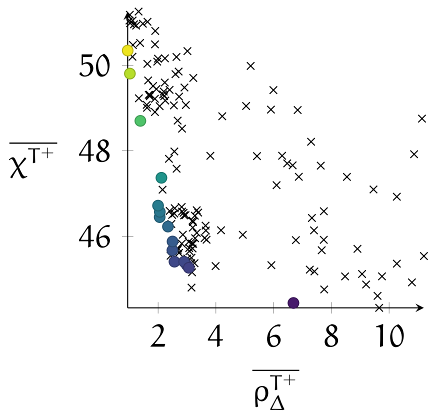

(b) density difference VS travel time

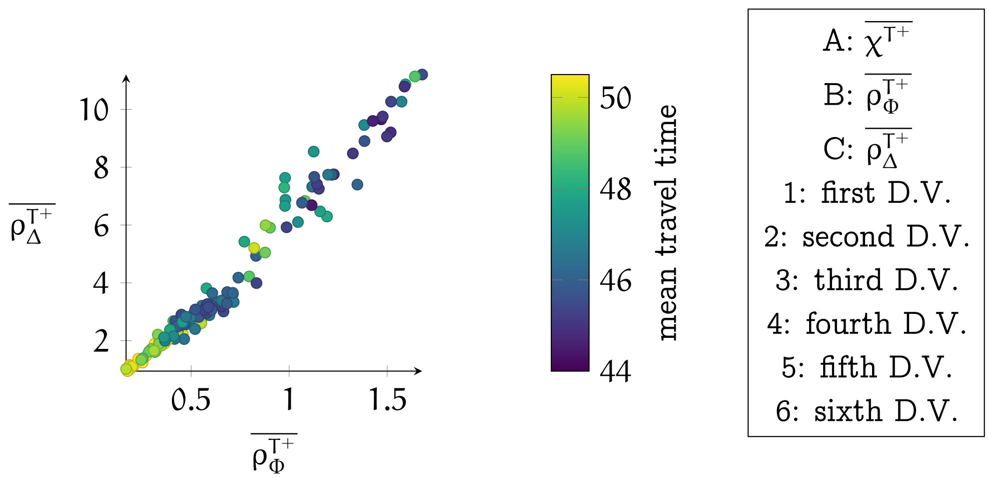

(c) density VS density difference and legend

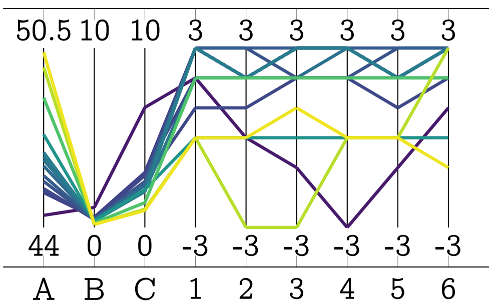

(d) MW-1 speed profiles.

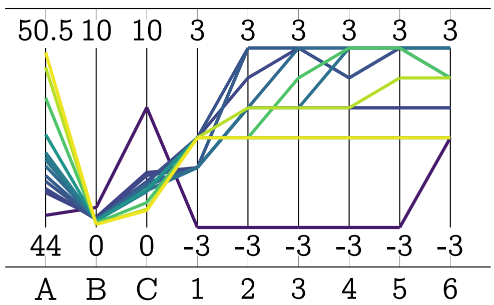

(e) AMW4 speed profiles.

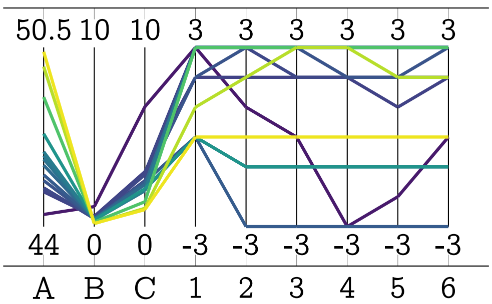

(f) MW-2 speed profiles.

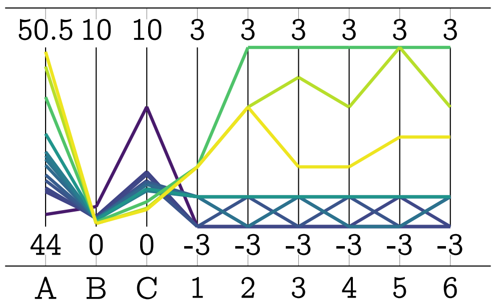

(g) MW-3 speed profiles.

Figure 19: Pareto frontier and AMW speed profiles for a low demand period (7:37 - 7:40).

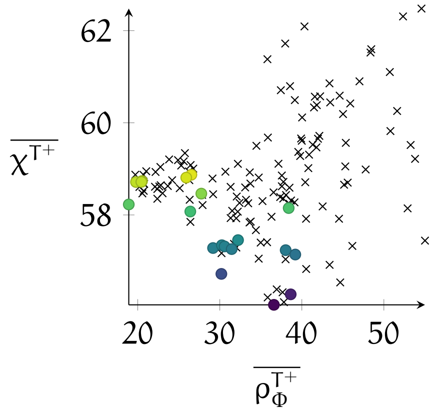

(a) density VS travel time

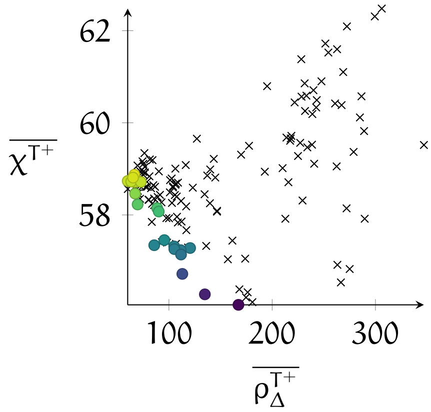

(b) density difference VS travel time

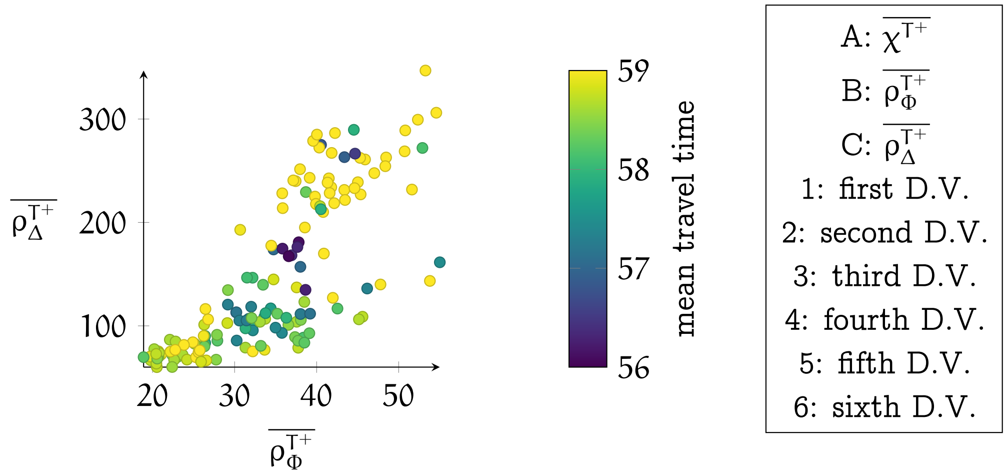

(c) density VS density difference and legend

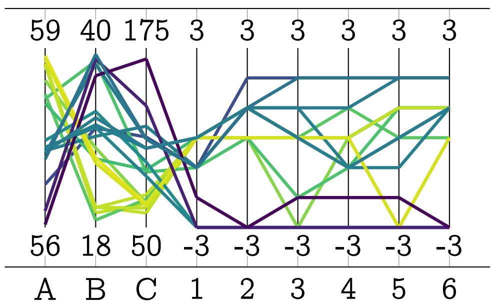

(d) MW-1 speed profiles.

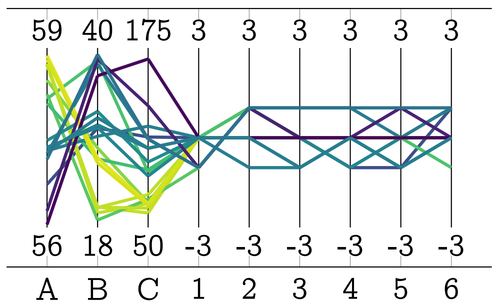

(e) AMW4 speed profiles.

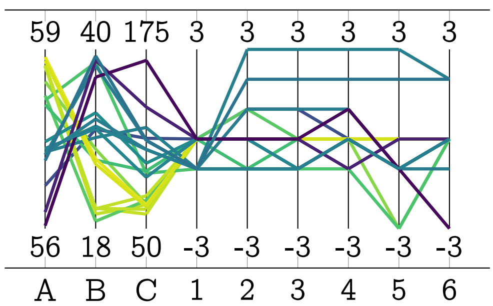

(f) MW-2 speed profiles.

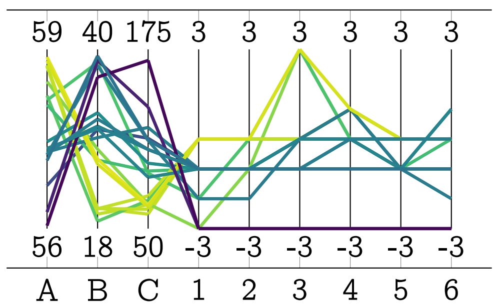

(g) MW-3 speed profiles.

Figure 20: Pareto frontier and AMW speed profiles for a high demand period (7:41:30 - 7:44:30).

7 Conclusion

With this paper, we addressed the question of dynamic control strategies for pedestrians. We proposed several variations of a control strategy which exploits existing pedestrian dedicated infrastructure. The usage of moving walkways as a control strategy is interesting since pedestrians have the habit of using them, hence there is no technology barrier to address. Furthermore, moving walkways address the problem of compliance since pedestrians cannot feasibly use them in the wrong direction.

The first hypothesis regarding the effectiveness of moving walkways to manage pedestrian flows has clearly been shown through both case studies. Although the fixed control algorithm produced poor results, the dynamic strategies effectively reduced pedestrian travel time and prevented excessive congestion in both case studies considered in this paper. Next, we have shown that a predictive algorithm can significantly improve pedestrian dynamics in more complex scenarios. Furthermore, the predictive flavour is generally fairer across different categories of pedestrians than the reactive algorithm. Finally, the advantages of considering multiple objectives (third hypothesis) in the optimization algorithm used by the predictive algorithm are emphasized when analysing the pareto set of solutions. The trade-off between travel time and congestion stands out and provides insight to the operator when decisions must be made.

The different responses to the dynamic control strategies of each case study emphasize the need for in depth analysis of the demand scenario and infrastructure configuration. Considering the challenge of integrating short term predictions into control strategies, effort should be invested in reactive strategies to develop more advanced control algorithms which could possibly reach similar benefits as the predictive algorithms. Identification of the scenario and contexts where reactive and predictive algorithms produce similar results should be done to better understand when short term predictions are needed.

Consolidation of these results with applications to different environments would provide further insights into the conditions where predictive algorithms are better than reactive ones. Exploring different demand structures and different walkable environments can help achieve this objective. The development of control strategies which are robust to measurement errors and biases is critical for real world applications. This should first be addressed in a simulation environment by using a different simulator for the ground truth and prediction simulators. In such a context, measurement errors, detector defects or biases can be simulated to develop a robust control strategy. Furthermore, the computational time of the short term predictions must be addressed. Practical considerations regarding compliance and safety should also be investigated prior to any full scale installations inside existing pedestrian infrastructure.

References

Abdelghany, A., Abdelghany, K., and Mahmassani, H. (2016). A hybrid simulation-assignment modeling framework for crowd dynamics in large-scale pedestrian facilities. *Transportation Research Part A: Policy and Practice*, 86:159 – 176.

Abuamer, I. M., Silgu, M. A., and Celikoglu, H. B. (2016). Micro-simulation based ramp metering on istanbul freeways: An evaluation adopting alinea. In *2016 IEEE 19th International Conference on Intelligent Transportation Systems (ITSC)*, pages 695–700.

Aros-Vera, F., Sadeghi, A., Younes Sinaki, R., and Sormaz, D. (2020). A simulation-based framework for checkpoint design in large-scale crowd management: Case study of the papal mass in philadelphia. *Safety Science*, 127:104701.

Baskar, L. D., De Schutter, B., Hellendoorn, J., and Papp, Z. (2011). Traffic control and intelligent vehicle highway systems: a survey. *IET Intelligent Transport Systems*, 5(1):38–52.

Bellemans, T., De Schutter, B., and De Moor, B. (2006). Model predictive control for ramp metering of motorway traffic: A case study. *Control Engineering Practice*, 14(7):757 – 767.

Ben-Akiva, M. and Bierlaire, M. (2003). *Discrete Choice Models with Applications to Departure Time and Route Choice*, pages 7–37. Springer US, Boston, MA.

Ben-Akiva, M., Cuneo, D., Hasan, M., Jha, M., and Yang, Q. (2003). Evaluation of freeway control using a microscopic simulation laboratory. *Transportation research Part C: emerging technologies*, 11(1):29–50.

Campanella, M. C. (2016). *Microscopic modelling of walking behaviour*. TRAIL.

Fonseca, F., Ribeiro, P., Jabbari, M., Petrova, E., Papageorgiou, G., Conticelli, E., Tondelli, S., and Ramos, R. (2020). Smart pedestrian network: An integrated conceptual model for improving walkability. In Pereira, P., Ribeiro, R., Oliveira, I., and Novais, P., editors, *Society with Future: Smart and Liveable Cities*, pages 125–142, Cham. Springer International Publishing.

Fruin, J. J. (1971). *Designing for pedestrians: A level-of-service concept*. Number HS-011 999.

Gendreau, M., Potvin, J.-Y., et al. (2010). *Handbook of metaheuristics*, volume 2. Springer.

Hoogendoorn, S. and Bovy, P. (2004). Pedestrian route-choice and activity scheduling theory and models. *Transportation Research Part B: Methodological*, 38(2):169 – 190.

Jiang, Z., Fan, W., Liu, W., Zhu, B., and Gu, J. (2018). Reinforcement learning approach for coordinated passenger inflow control of urban rail transit in peak hours. *Transportation Research Part C: Emerging Technologies*, 88:1 – 16.

Liu, R., Li, S., and Yang, L. (2020a). Collaborative optimization for metro train scheduling and train connections combined with passenger flow control strategy. *Omega*, 90:101990.

Liu, Y., Yang, D., Timmermans, H. J., and de Vries, B. (2020b). The impact of the street-scale built environment on pedestrian metro station access/egress route choice. *Transportation Research Part D: Transport and Environment*, 87:102491.

Molyneaux, N., Scarinci, R., Bierlaire, M., et al. (2019). Design and analysis of control strategies for pedestrian flows. *Transportation*, pages 1–41.

Mulholland, M. (2016). *Applied process control : essential methods*. Wiley-VCH, Weinheim.

Nikolić, M., Bierlaire, M., Farooq, B., and de Lapparent, M. (2016). Probabilistic speed–density relationship for pedestrian traffic. *Transportation Research Part B: Methodological*, 89:58 – 81.

Papageorgiou, M., Diakaki, C., Dinopoulou, V., Kotsialos, A., and Wang, Y. (2003). Review of road traffic control strategies. *Proceedings of the IEEE*, 91(12):2043–2067.

Papageorgiou, M., Hadj-Salem, H., Blosseville, J.-M., et al. (1991). Alinea: A local feedback control law for on-ramp metering. *Transportation Research Record*, 1320(1):58–67.

Prato, C. G. (2009). Route choice modeling: past, present and future research directions. *Journal of Choice Modelling*, 2(1):65 – 100.

Roncoli, C., Papamichail, I., and Papageorgiou, M. (2016). Hierarchical model predictive control for multi-lane motorways in presence of vehicle automation and communication systems. *Transportation Research Part C: Emerging Technologies*, 62:117 – 132.

Ropke, S. and Pisinger, D. (2006). An adaptive large neighborhood search heuristic for the pickup and delivery problem with time windows. *Transportation science*, 40(4):455–472.

Scarinci, R., Markov, I., and Bierlaire, M. (2017). Network design of a transport system based on accelerating moving walkways. *Transportation Research Part C: Emerging Technologies*, 80:310–328.

Seriani, S. and Fernandez, R. (2015). Pedestrian traffic management of boarding and alighting in metro stations. *Transportation Research Part C: Emerging Technologies*, 53:76 – 92.

Shang, P., Li, R., Guo, J., Xian, K., and Zhou, X. (2019). Integrating lagrangian and eulerian observations for passenger flow state estimation in an urban rail transit network: A space-time-state hyper network-based assignment approach. *Transportation Research Part B: Methodological*, 121:135 – 167.

Tang, T.-Q., Yi, Z.-Y., Zhang, J., Wang, T., and Leng, J.-Q. (2018). A speed guidance strategy for multiple signalized intersections based on car-following model. *Physica A: Statistical Mechanics and its Applications*, 496:399 – 409.

Tympakianaki, A., Spiliopoulou, A., Kouvelas, A., Papamichail, I., Papageorgiou, M., and Wang, Y. (2014). Real-time merging traffic control for throughput maximization at motorway work zones. *Transportation Research Part C: Emerging Technologies*, 44:242 – 252.

Wang, L., Zhang, Q., Cai, Y., Zhang, J., and Ma, Q. (2013). Simulation study of pedestrian flow in a station hall during the spring festival travel rush. *Physica A: Statistical Mechanics and its Applications*, 392(10):2470 – 2478.

Xu, X.-Y., Liu, J., ying Li, H., and Jiang, M. (2016). Capacity-oriented passenger flow control under uncertain demand: Algorithm development and real-world case study. *Transportation Research Part E: Logistics and Transportation Review*, 87:130 – 148.

Zhang, Z. and Jia, L. (2021). Optimal feedback control of pedestrian counter flow in bidirectional corridors with multiple inflows. *Applied Mathematical Modelling*, 90:474 – 487.

Zhang, Z., Jia, L., and Qin, Y. (2016). Level-of-service based hierarchical feedback control method of network-wide pedestrian flow. *Mathematical Problems in Engineering*, 2016.

Zhou, M., Yu, Y., and Qu, X. (2020). Development of an efficient driving strategy for connected and automated vehicles at signalized intersections: A reinforcement learning approach. *IEEE Transactions on Intelligent Transportation Systems*, 21(1):433–443.